

**MATHEMATICAL MODELLING AND SIMULATION OF SOLID  
OXIDE FUEL CELL AND GAS TURBINE HYBRID SYSTEM FOR  
ENHANCING THERMAL PERFORMANCE**

**Thesis submitted in partial fulfillment of the Requirements for  
the Award of the Degree of**

**“MASTER OF TECHNOLOGY IN THERMAL  
ENGINEERING”**

**By**

**SMITA SHARMA**

**(2K14/THE/21)**

**Under the supervision of**

**Prof. (Dr.) R. S. MISHRA**



**DEPARTMENT OF MECHANICAL ENGINEERING,  
DELHI TECHNOLOGICAL UNIVERSITY (DTU),  
SHAHBAD DAULATPUR, MAIN BAWANA ROAD,  
DELHI, INDIA**

**JUNE- 2016**



**Department Of Mechanical Engineering  
Delhi Technological University (DTU)  
Delhi-110042**

## **CERTIFICATE**

This is to certify that the project titled “**Mathematical Modelling and Simulation of Solid oxide fuel cell and Gas turbine Hybrid system for enhancing Thermal Performance**” is a bonafide record of the work carried out by **Mrs. Smita Sharma**, Roll No. 2K14/THE/21, under my supervision and guidance for the partial fulfilment of the requirements for the degree of Master of Technology in Thermal Engineering specialization during the academic session 2014-2016 in the Department of Mechanical Engineering, Delhi Technological University, Delhi.

Date:

**Dr. R. S. Mishra**

**(Professor and Head of Department)**

Place: Delhi

Department of Mechanical, Production &  
Industrial and Automobiles Engineering  
Delhi Technological University, Delhi-42



**Department Of Mechanical Engineering  
Delhi Technological University (DTU)  
Delhi-110042**

### **CERTIFICATE OF EXAMINATION**

This is to certify that we have examined the thesis entitled **“Mathematical Modelling and Simulation of Solid oxide fuel cell and Gas turbine Hybrid system for enhancing Thermal Performance”** submitted by **Mrs. Smita Sharma**, Roll no. 2K14/THE/21, a post graduate student of Mechanical Engineering Department with specialization Thermal Engineering. We here by accord our approval of it as a study carried out and presented in a manner required for its acceptance in partial fulfilment of the requirements for the degree of Master of Technology in Thermal Engineering specialization for which it has been submitted. This approval does not necessarily endorse or accept every statement made, opinion expressed or conclusion drawn as recorded in this thesis. It only signifies the acceptance of the thesis for the purpose for which it is submitted.

Supervisor:

Head of Department

## ACKNOWLEDGEMENT

Generally, individuals set aims, but more often than not, their conquest are by the efforts of not just one but many determined people. This complete project could be accomplished because of contribution of a number of people. I take it as a privilege to appreciate and acknowledge the efforts of all those who have, directly or indirectly, helped me achieving my aim.

I take great pride in expressing my unfeigned appreciation and gratitude to my learned mentor **Prof. R. S. Mishra**, Head, Department of Mechanical Engineering, for this invaluable inspiration, guidance and continuous encouragement throughout this project work. His critics and suggestions on my project work have always guided me towards perfection. This work is simply the reflection of their thoughts, ideas, concepts and above all his efforts. Working under his guidance has been a privilege and an excellent learning experience that I will cherish for a long time.

I would like to thank all faculty members of the department who have been extremely kind and helpful to me during my M Tech and motivated me from time to time to perform my level best.

I would like to thank my lucky stars for such wonderful, kind and understanding life partner who always encouraged me to get best out of my capabilities.

Lastly I would like to express my gratitude to this great institute, which gave me this opportunity to learn.

Date:

Smita Sharma  
(Roll No. 2K14/THE/21)

## **ABSTRACT**

Fuel cell systems are environment friendly. It is a clean energy generator but it has a low efficiency when it is used alone. Gas turbine also has a lower efficiency around 30% when working alone. Hybrid system is the combination of gas turbine and fuel cell to achieve a higher efficiency around 60-70%. The fuel cell generates the major portion of the plant power output and the gas turbine generates a fraction of total power output. The major advantage of fuel cell is that it is not a heat engine so its efficiency can be 100 % as it is not limited by the Carnot efficiency.

This Thesis work includes development of mathematical model and simulation of a Solid oxide fuel cell combined with gas turbine hybrid system using Methane as a fuel. This type of hybrid system has a wide application such as decentralised electricity supply in houses and buildings, heat and cooling energy. With the developments in the technology of commercialized fuel cell the system can be used in centralized power plant.

Program is developed to simulate this developed model. Power output, First law efficiency and second law efficiency is calculated from the simulation of the developed model. The calculated Power output is 1.488 MW, first law efficiency is 66.25 % and second law efficiency is 63.23 %.

<b>CONTENT</b>	<b>PAGE NO.</b>
Nomenclature	viii
List of Figures	x
List of Tables	xii
<b>1. Introduction</b>	<b>1-3</b>
1.1 Introduction of Hybrid system	1
1.2 Motivation behind the present work	2
1.3 Objective of the Work	2
1.4 Structure of thesis	3
<b>2. Literature Review</b>	<b>4-11</b>
2.1 Literature reviews of Gas turbine, Fuel cell and fuel cell/ gas turbine hybrid system	4
2.2 Conclusions from Literature review	10
2.3 Research gap identified and present investigation	11
<b>3. Modelling of Gas Turbine</b>	<b>12-17</b>
3.1 Introduction	12
3.2 Modelling of Components of gas turbine power plant	12
<b>4. Modelling of fuel cell</b>	<b>18-37</b>
4.1. Introduction of Fuel cell	18
4.2 Types of fuel cells	19
4.3 Solid oxide fuel cell (SOFC)	21
4.4 Types of Solid oxide fuel cell design	22
4.5 Electrochemical reaction	24
4.6 Stacking of Fuel cell	24
4.7 Faraday's Law for fuel cell	25
4.8 Efficiency related terms	26
4.9 Cell voltage related terms	27
4.10 Nernst Voltage	28
4.11 Losses in terms of voltage in a fuel cell	29
4.12 Polarization Curve	34
4.13 Cell Power output	35
4.14 Exergy analysis of Fuel cell	35
4.15 Environmental Impact of SOFC	37

<b>5. Modelling of SOFC/GT Hybrid system</b>	<b>38-47</b>
5.1 Introduction	38
5.2 Hybrid system types	38
5.3 Application of Hybrid system	42
5.4 System selection for Analysis	43
<b>6. Result and Discussion</b>	<b>48-63</b>
6.1 Program validation	48
6.2 Exergy destruction in various components	50
6.3 Thermal analysis based upon the simulation	51
<b>7. Conclusion</b>	<b>64</b>
<b>8. Recommendation and Scope of Future Work</b>	<b>65</b>
<b>References</b>	<b>66-70</b>
<b>Appendix A</b>	<b>71</b>
<b>Appendix B</b>	<b>72-78</b>

## **NOMENCLATURE**

$A_t$	Total active surface area of cell ( $m^2$ )
$A_c$	surface area of one cell ( $m^2$ )
$D_{Eff}$	Effective diffusion coefficient
$E$	Nernst Voltage (V)
$E^0$	Maximum expected voltage (V)
$E^{00}$	Thermal voltage (V)
$F$	Faraday's constant (96485 C/eq)
$I_{oa}$	Exchange current density for anode ( $A/m^2$ )
$i_L$	Limiting Current density ( $A/m^2$ )
$I$	Cell current (A)
$J$	Current density ( $A/m^2$ )
$MW$	Molecular weight
$n_e$	Number of electron passing per mole species
$\dot{n}_x$	Molar flow rate of consumption or production(mol/s)
$N_{Stack}$	No. of stack
$N_{cell}$	Number of cell
$N_{cell}^{stack}$	Number of cell per stack
$P_{el}$	Electrical power (kW)
$q$	Charge passed per mol of species
$R$	Resistance ( $\Omega$ )
$R_u$	Universal gas constant
$T$	Temperature (K)
$V_{cell}$	Cell voltage (V)
$V_{stack}$	Stack voltage (V)
$\eta_{aano}$	Activation loss at anode (V)
$\eta_{acat}$	Activation loss at cathode (V)
$\eta_{cano}$	Concentration loss at anode (V)
$\eta_{ccat}$	Concentration loss at cathode (V)
$\eta_{Ohm}$	Ohmic Loss (V)
$\eta_x$	Species cross over losses (V)
$U_f$	Fuel utilization efficiency (%)
$\delta$	Diffusion layer thickness (m)



$\rho$  Resistivity

$\eta_{th}$  Thermodynamic cell efficiency

### **Subscript / Superscript**

AC: Alternating current

DC: Direct current

e:Electrons

eff: Effective

GT: Gas turbine

max: maximum

MGT: Micro gas turbine

MW: Megawatt

CHP: Combined heat and power

cell: Fuel cell

SOFC: solid oxide fuel cell

TSOFC: tubular solid oxide fuel cell

PSOFC: Planer solid oxide fuel cell

TIT: turbine inlet temperature

## LIST OF FIGURES

<b>Figure No.</b>	<b>Title</b>	<b>Page No.</b>
<b>3.1</b>	Schematic diagram of Gas turbine	13
<b>4.1</b>	Fuel Cell	18
<b>4.2</b>	Methods of conversion of chemical energy into electrical energy	19
<b>4.3</b>	Design of fuel cell	23
<b>4.4</b>	Electrochemical reaction in fuel cell	24
<b>4.5</b>	Polarization curves	34
<b>4.6</b>	Variation of Ohmic loss with current density	35
<b>5.1</b>	Indirect Integration hybrid systems	39
<b>5.2</b>	Direct Integration hybrid systems	41
<b>5.3</b>	Hybrid systems selected for analysis	43
<b>6.1</b>	Variation of Cell operating voltage with current density	52
<b>6.2</b>	Variation of Activation loss with current density	52
<b>6.3</b>	Variation of Ohmic loss with current density	53
<b>6.4</b>	Variation of Concentration loss with current density	53
<b>6.5</b>	Variation of Power density and voltage with current density	54
<b>6.6</b>	Variation of Efficiency with current density	54
<b>6.7</b>	Variation of Cell AC power with current density	55
<b>6.8</b>	Variation of Turbine work with Fuel flow	56

<b>6.9</b>	Variation of Cell AC power with Fuel flow	56
<b>6.10</b>	Variation of Hybrid system efficiency with Fuel utilization efficiency	57
<b>6.11</b>	Variation of Hybrid system efficiency with Cell operating temperature	58
<b>6.12</b>	Variation of Power output with Cell operating temperature	58
<b>6.13</b>	Variation of Hybrid system efficiency with Pressure ratios	60
<b>6.14</b>	Variation of Cell power output with Pressure ratios	60
<b>6.15</b>	Variation of Cell voltage with Pressure ratios	61
<b>6.16</b>	Variation of Turbine power output with Pressure ratios	61
<b>6.17</b>	Variation of exergy efficiency with Pressure ratios of compressor	62
<b>6.18</b>	Variation of exergy destruction in SOFC and CC with Pressure ratios of compressor	62
<b>6.19</b>	Variation of First law efficiency with turbine inlet temperature	63
<b>6.20</b>	Variation of exergy efficiency with turbine inlet temperature	63

## LIST OF TABLES

<b>Table</b>	<b>Title</b>	<b>Page No.</b>
<b>4.1</b>	Fuel cell Types, Description and Basic data	20
<b>5.1</b>	State points and abbreviation for Indirect integration hybrid system	40
<b>5.2</b>	State points and abbreviation for direct integration hybrid system	41
<b>5.3</b>	State points and abbreviation for selected hybrid system configuration for analysis	44
<b>5.4</b>	Flow information for hybrid system selected for analysis	45
<b>5.5</b>	Standard molar chemical exergy (kJ/kmol) of various substance at $T_0$ (298.5 K) and $P_0$ (1.01325 bar)	46
<b>5.6</b>	Input Parameters	47
<b>6.1</b>	Results	48
<b>6.2</b>	Various output parameters obtained for each state point thermodynamic properties from execution of programme	49
<b>6.3</b>	Exergy Destruction in various components	50
<b>A.1</b>	Resistivity Constant	71
<b>A.2</b>	Fuller diffusion volume	71

# CHAPTER-1

## Introduction

### 1.1 Introduction of Hybrid system

There is ongoing crisis of energy due to increase in uses of fuels and diminishing fossil fuels resources. The another factor is environmental issues related to pollutant emission and global warming due to which people should pay more attention about renewable energy sources and other alternative resources which has high energy conversion efficiency. Fuel cells have high potential for energy conversion and to satisfy future needs of energy. Fuel cell has following advantages:

- i) Operation is quiet and simple as there is no moving or rotating part
- ii) Pollution is less
- iii) Conversion efficiency is High
- iv) System is compact
- v) Charging is not required
- vi) Can be used from 50% to 100% load
- vii) Modular in nature
- viii) Flexibility in fuel is possible
- ix) No transmission and distribution losses
- x) Heat generated can be used locally
- xi) Fuel cell can be used with turbine to form a hybrid system to increase power output.

With the advancement in the development of the commercial fuel cell they will preferably be used in various applications such as:

- i) It can be used for power load levelling.
- ii) Fuel cell can be used in central station power plant resulting high efficiency with reduced emissions.
- iii) Used in distributed power generation.
- iv) In hospital, vehicles, submarine, spacecraft, mobile phones and other low power appliances.

An extensive research in the field of combined fuel cell and gas turbine hybrid system is going on. This type of hybrid system uses a gas turbine and a high temperature fuel cell to achieve higher efficiency and overall performance than an Individual power plant. Heat can be recovered from the high temperature exhaust gas from the fuel cell which further

used to drive gas turbine. In the gas turbine exhaust gases expand and produces additional power.

This hybrid system is a combination of two systems. One is gas turbine which acts as a heat engine. The other one is fuel cell which is a non heat engine. The efficiency and the overall performance of this hybrid system are far better than provided by individual system working alone. Basically in this hybrid system coupling of fuel cell and gas turbine is performed for power generation. Coupling can be performed by two methods:

1. Indirect method
2. Direct method

## **1.2 Motivation behind the present work**

A clean method of power generation is electrochemical extraction of energy from hydrogen via fuel cell. This technology is very promising technology for post fossil fuel related energy economy. But the process of transition from the fossil fuels to hydrogen based systems is very complex in nature and it will take time. There are various types of fuel cell in which solid oxide fuel cell is well suited. The operating temperature of SOFC is very high which facilitates combination of SOFC with steam and gas turbine to achieve a higher electrical efficiency which is beyond the limitations related to conventional technologies. Fuel cell is well suited for distributed power generation as it can achieve higher efficiency even for small units. The experimental investigation of such a hybrid system for evaluation of thermal performance is very expensive. A mathematical model of the system is helpful in this respect. Simulation of the system on computer can be performed based on the mathematical model developed and it is easy and inexpensive.

## **1.3 Objective of the Work**

Though Fuel Cell /Gas Turbine hybrid systems are very promising, studies on mathematical modelling and simulation of these systems are relatively few. Therefore the objective of the present work is to develop a mathematical model and simulate a SOFC/GT hybrid system. Computer programme for simulation of the model has been developed.

The present work has following objectives:

- i. To find out best configuration of SOFC/GT hybrid power generation system from the available configuration.
- ii. Mathematical modelling of this hybrid plant using methane as fuel
- iii. Simulation of the hybrid plant.
- iv. Performance evaluation of the hybrid plant is carried out.
- v. To find out first and second law efficiency.

## **1.4 Structure of thesis:**

**In chapter 1** introduction of gas turbine, fuel cells and hybrid systems is discussed in brief and explain the reason of motivation and finally the objective of the thesis work is discussed.

**In chapter 2** a brief review of literature relevant to gas turbine, fuel cell and hybrid system are discussed. These literatures give the detailed explanation of the advancement and development in the field of gas turbine, fuel cell and hybrid system. After detailed discussion about literature review a conclusion is drawn from it.

**In chapter 3** Introduction of Gas turbine power plant is presented. After that mathematical modelling of all components in a gas turbine power generation plant are done one by one. Each component of the plants such a compressor, combustion chamber and the gas turbine etc. is modelled with given assumptions.

**In chapter 4** A detailed introduction of fuel cell is presented. This includes introduction of fuel cell, fuel cell types and then the detailed explanation of solid oxide fuel cell. Formulation of fuel cells is carried out which is used in the mathematical modelling to evaluate the thermal performance of the cell.

**In chapter 5** Introduction of hybrid systems is discussed. Methods of coupling of gas turbine with fuel cell are also explained. Selection of system is performed for the thesis work. System model for analysis has been discussed.

**In chapter 6** the system model which is developed is simulated and simulation results are produced. Analysis of system is performed.

**In chapter 7** Conclusions from the modelling and simulation work are presented.

**In chapter 8** Scope of future work related to the Hybrid system are explained.

# CHAPTER 2

## Literature review

Fuel cell/Gas turbine hybrid power generation plant has wide range of applications. Both gas turbines and fuel cells systems are very extensive field of research. Many research have already been done and many more to go. For the sake of the simplicity this literature review is discussed in three parts. First part explain the literature reviews related to gas turbine, second part about fuel cell and the third one about hybrid system. A large body of numerical and experimental works exists on the various aspects of these systems. Some of these are reviewed here.

### **2.1 Literature reviews of Gas turbine, Fuel cell and fuel cell/ gas turbine hybrid system**

Power production from Gas turbines is very common now days. Gas turbine is used from a very long time. Power for jet aircrafts and industrial power in power plants are produced by the gas turbine. The gas turbine is a device which converts the chemical energy of fuel into the mechanical energy. Working principle of the Gas turbine is similar to a combustion engine. The working fluid cycle in gas turbine such as air cycle is like a combustion engine fluid cycle. Air is compressed then fuel is added. After mixing the air and fuel, Combustion process is initiated by ignition. In the combustion process energy releases and physical barrier moves with the expansion of the fluid. This movement of barrier gives Mechanical work output of the cycle. In the next coming cycle, a small portion of this mechanical energy is being used to compress working fluid. The main difference between these two is that combustion engine cycle has iterative cycles whereas gas turbine working cycle runs continuously. Air Compressor, combustor and gas turbine these are the main components of the gas turbine power plant [1]. An investigation of chemically recuperated GT power plant (CRGT) was done. A computer code was generated for evaluating specific work and the thermal efficiency. The comparison of this GT plant with the other power plant such as gas turbine plant injected by steam (STIG), gas turbine plant with combined cycle (CC) and gas turbine plant with simple cycle plant (SC) was performed. The comparison result explains that the thermal efficiency of CRGT is higher in comparison to both STIG and SC



but it is lower than CC [2]. Whenever the comparison of the features of gas turbine and steam turbine is performed it is clear that gas turbine has many attractive features such as (I) It has low capital cost (ii) Compact size (iii) Short delivery (iv) High flexibility (v) Reliability (vi) Fast starting (vii) Fast loading (viii) Needs of operating manpower is less (ix) better environmental performance. It has some disadvantages also such as limited efficiency at part load. Cogeneration is a technology in which the demerits of the gas turbine can be removed by combining the gas turbine with steam turbine so that overall improved thermal efficiency will be obtained with the good features which are already available in the gas turbine. It is the technology in which heat energy of the exhaust gas is utilized with the production of power and efficiency otherwise wasted [3]. Efficiency of gas turbine plant could be enhanced by reducing the air temperature at turbine inlet. Air cooling was performed by a pre-cooler installed at air inlet which was connected with an evaporator of absorption chiller system using aqua ammonia as a working fluid. That chiller system was driven by the heat of exhaust gases recovered from tail-end from the engine. A boiler was used with the intention of exhaust heat part recovery before it enters into the generator of chiller system. The three main performance parameters namely power output, thermal efficiency and the specific fuel consumption of that combined cycle was compared with simple cycle. The main variable taken in the parametric analysis was (i) Compressor pressure ratio (ii) Turbine inlet temperature (TIT) (iii) ambient temperature. The analysis reveals that there was a gain achieved in the combined system. Results are as follows: (i) gain in power is 21.5% (ii) gain in overall efficiency is 38% (iii) gain in overall fuel consumption is 27.7% (iv) Performance of combined system was less sensitive to variation in the operating variables [4]. When the comparison was performed between combined cycle and Gas turbines which uses mixture of air and water as working fluid the result shows: (i) Gas turbine provide higher value of electrical efficiencies (ii) gas turbine provide higher specific output power (iii) lower specific investment cost. Due to these advantages various types of humidified gas turbine were proposed such as (i) Direct water-injected cycles (ii) Steam-injected cycles (iii) Evaporative cycles having humidification towers. However the implementation of few of these types of humidified gas turbine was becomes possible and very less of them were commercially available. The process of injection of water and steam increases the flow rate of the turbine due to which the specific power output increases [5]. One of the methods of increasing the thermal efficiency of the gas turbine is to utilize the heat of gas turbine exhaust stream by installing a recuperator which is also

called a heat exchanger. It transfer the heat of turbine exhaust stream to the air at combustor inlet consequently: (ii) It increases combustion inlet air temperature (iii) Reduces the quantity of fuel required to obtain the desired turbine inlet temperature (iii) Specific fuel consumption is also reduced as compared to simple cycle (iv) It also ensure that the exhaust temperature can be used for combined power generation. Gas turbine cycles having with heat recovery system are generally recognized as advanced cycle. By using heat recovery system the efficiency of plant can be increased above 40%. It was also observed that for given electricity output there was a lower emission of pollutant [6]. The Pilavachi [6] had discussed few examples of developments/modifications in the gas turbine to achieve a higher efficiency from gas turbine which were as follows: (i) increased TIT (ii) waste heat recuperation (iii) steam or water injection (iv) Combined cycle etc. SOFC is considered as most promising technology since last few years. It is known for its high efficiency electricity generation using natural gas either in a simple fuel cell power plant or in Hybrid system with gas turbine. Various geometry of fuel cell is popular but the most mature geometry is tubular SOFC with internal reforming which has the possibility of commercialization. A model was calibrated on the basis of available data for a demonstrated tubular Solid oxide fuel cell prototype plant. The analysis results of thermodynamic and parametric study yield a very useful consideration for (i) partial load operation (ii) load regulation (iii) design of system and integration of fuel cell with gas turbine [7].

Two computational models were developed for electrical performance of tubular SOFC system. Design of tubular SOFC was taken from Siemens Westinghouse Corporation. Results of both two methods were matching with the performance results quoted experimentally. A simple analytical procedure could also be used for the performance prediction of cell which is the function of cell dimension [8]. An empirical model for the PEM fuel cell was presented to simulate its performance without extensive calculations. An investigation was done to observe the variation in design optimization with varying operating conditions [9]. An analysis was carried out using cryogenic hydrogen fueled integrated SOFC and GT system. Mass of component was estimated. Two designs of SOFC were compared. The dependence of system at the time of take-off on the SOFC operating condition is investigated. Results conclude that the system has higher efficiency with lower mass in comparison to other comparable systems [10]. The SOFC system is most promising system for conversion of the chemical energy of fuel into the electrical energy.

Due to High temperature of exhaust stream it can be used for cogeneration. The operating temperature range of SOFC is 600–1000°C. At this temperature range ceramic electrolyte in fuel cell Conduct oxygen ions while act as nonconductive to electrons. For modeling of a fuel cell detailed reviews of modeling approaches were explained [11]. One of the analytical models of a micro SOFC system using butane as fuel is presented and analysis was performed to optimize the exergetic efficiency. The operational performance of a Micro SOFC plant is calculated by using operational parameters. The parameters considered in the calculations were taken from the experimental results of the previous studies [12]. A device which produces electricity by direct conversion of chemical energy of fuel is called fuel cell. The fuel cell is not undergoing any combustion process. There is only electrochemical process during which electricity produced. This technology is very promising and suitable for integration with renewable energy schemes. Fuel cell has an advantage of developing high efficiency in part load as well as in full load application. Due to this reason it is a promising technology for producing electrical power in stationary power sector. It has various advantageous features such as (i) produce electricity without combustion (ii) Produce electricity without rotating machinery (iii) Can be utilized with cogeneration to generate power output and thermal energy (iv) Low pollution level [13]. The effect of various parameters on the efficiency of SOFC system was studied. These parameters are (i) air to fuel ratio (A/F) (ii) fuel utilization (iii) pre-reforming rate [14]. Fuel cell technology shows the fuel flexibility and modularity. It is almost free from problems such as (i) lubrication (ii) wear (iii) leakage (iv) heat loss. Generally hydrogen is used as fuel due to its high electrochemical activity. Carbon monoxide can also be used as fuel along with hydrogen [15]. To predict performance of proton exchange membrane type of fuel cell for engineering application a semi empirical model was developed. Semi empirical equations were used to develop the model. The empirical coefficients were calculated using linear least squares. This developed model was used in the performance evaluation of small distributed electricity generation systems. It was also used for the designing fuel cell systems applicable for vehicle and portable electronics [16]. An investigation was performed by taking biomass syn-gas as a fuel in a high temperature SOFC stack. Operation and performance for biomass gasification CHP plant were studied. Tubular SOFC configuration which was designed by Siemens Power Generation Inc (SPGI) was selected. It was considered the most superior design and is best suited for future commercialization. A computer simulated model of SPGI (100 kW AC CHP) for Tubular SOFC was developed

using software Aspen Plus. The optimum net electrical efficiency ranging between 36.1% - 37.8 % was observed [17]. The performance of PEM fuel cell using hydrogen as fuel is measured experimentally by varying air flow rate and operating temperature. The comparison of result obtained was done with the experimental data of 40 watt PEM fuel cell and it is found to be matching with it [18]. PEM fuel cell system operates at a lower temperature range of 60-120°C. It is applicable in various areas such as (i) transportation (ii) demonstration (iii) small power applications in the range of 5-250 kW [19].

A hybrid system in which fuel cell contributed  $\frac{3}{4}$  portions (149 kW) and gas turbine contributed  $\frac{1}{4}$  portions (50kW) of the total power generation was studied. It was calculated that the total system efficiency of this hybrid system was 43.4% [20]. A 30 kW SOFC/GT hybrid system which was conceptually designed for a small distributed energy systems was investigated. System characteristic at design and part load was investigated. After this investigation part load operational performance has been evaluated in 2 different modes. One is constant rotation speed and another is variable rotation speed of gas turbine. The investigation Result shows that in these 2 modes, variable speed mode was more advantageous than constant speed mode for the performances degradation under the condition of part load [21]. The probabilistic analysis was done for field performance of gas turbine. Calculation of (i) The overall efficiency (ii) total specific power output of the hybrid SOFC-GT system was performed by applying control volume approach, 1<sup>st</sup> and 2<sup>nd</sup> law of thermodynamics. Results were presented as follows: (i) 64.1 % of thermal efficiency at 14 pressure ratio (ii) Specific power output was 520 W/kg s. [22]. A novel concept of integration of desalination systems with fuel cells was proposed and investigated. The 2 unique cases were discussed (i) having reverse osmosis (RO) (ii) hybrid system coupled with thermal desalination process like multi stage flash (MSF). The desalination unit utilized the exhaust gases from a hybrid power plant. Results indicated that these types of hybrid systems could show an increase of 5.6% of global efficiency [23]. Hybrid fuel cell gas turbine (FC/GT) systems are very advanced systems that produce electricity with ultra low emissions and higher efficiency for wide ranges of power plants sizes. A dynamic model of integrated SOFC/GT system was developed. Results and related experimental data were gathered for the period of operation along with testing of 220 kW. Hybrid SOFC/GT system were compared and presented at the National Fuel Cell Research Center [24]. A model of SOFC-GT hybrid system of 1.25 MW capacity using methane as fuel was successfully developed.

It was presented that the net efficiency of hybrid system is 60 percent and this can be improved further by installing a recuperator at the tail end of gas turbine [25]. A simulation methodology is presented for a small scale fuel cell using biogas as fuel for power generation. Efficiency of a simple gas turbine cycle, regenerating gas turbine cycle and SOFC cycle were compared and it was found that SOFC had superior efficiency for selected electrical power ranges [26]. SOFC stacks systems are very efficient for dispersed power generation sector. These systems are in development stages. The demand of fuel cell in various sectors makes it complicated configuration. SOFC plants for stationary application are generally connected to other component and subsystems like gasifier with (i) gas cleaning section (ii) a gas turbine (iii) heat recovery system, either for cogeneration or for added power production [27]. Power productions from GT power plant working on Brayton cycle suffer from many problems such as low efficiency, low fuel- power conversion. A SOFC system was proposed for coupling with a 10 MW GT plant operating at 30 percent efficiency with the aim of improving system efficiency and economy. The indirect coupling was done to minimize any disruption in GT operation. A thermo economic model was developed for a hybrid plant. The result shows a higher efficiency (49.9 percent) along with higher power output (20.6 MW) in comparison to single GT power plant [28]. Study of three combined heat - power system which was based on biomass gasification was presented at system level. These were classified on the basis of conversion of product gases into other system. These were as follows: (i) conversion into micro gas turbine (MGT) (ii) Product gas was converted into in a solid oxide fuel cell (SOFC) (iii) converted into hybrid system. A SOFC electrochemical model had been developed and calibration was performed with data published from Topsoe Fuel Cells A/S and the Risø National Laboratory. Study concluded that conversion of syn-gas by SOFC was more efficient than MGT. Unconverted remaining syn-gas from SOFC could be utilized in integrated SOFC/MGT system to produce additional power and the pressurized SOFC gives improved efficiency of 50.3% [29]. When a high temperature fuel cell is integrated with micro turbine, the resulting hybrid system always offers: (i) high efficiency (ii) low environmental pollution (iii) also can be used as a CHP producing both of heat and electricity in 2 modes-Grids Connected and Stand Alone. It was observed that in both modes the electrical efficiency could reach a high value (about 60%) and the total efficiency could be more than 70% which includes contribution of heat recovery. The steady state simulation was performed and result was found that efficiency of both the hybrid system and electrochemical system was

higher than the conventional gas turbine power plant and the steam turbine power generation plant [30]. For a SOFC-MGT hybrid system, the operating temperature of SOFC and inlet temperature of turbine are the main parameters which affect the operation performance of hybrid system. Author had proposed a least square (LS) support vector machine (.SVM) a type of identification model which was based on improved version of particle swarm optimization (PSO) to describe nonlinear dynamic temperatures properties of hybrid system. Parameters were optimized using improved PSO algorithm. For the prediction of data related to this model a physical model of SOFC/GT was established through Simulink toolbox of software MATLAB 6.5. Simulation results performed comparison between standard LS-SVM and conventional BP neural networks and predict that modified LS-SVM can efficiently imitate the temperature responses of the hybrid system [31].

## **2.2 Conclusions from Literature review**

Solid Oxide fuel cell is a clean energy source and it operates very efficiently for power generation. SOFC is best suited for distributed power generation in intermediate and long term future. Its high operating temperature (800-1100 K) allows fuel flexibility (including CO), ranging from few kW to MW. SOFC's are best suited for power generation with the integration of gas turbine system resulting into an efficient hybrid system. The hybrid system offers a high electrical efficiency of 60-70%.

Increasing interest in field of hybrid system which combine gas turbine and solid oxide fuel cell for power generation required an accurate mathematical modelling and computer simulation of system for its design and for evaluating performance at different conditions.

### **2.3 Research gap identified and present investigation**

From literature reviews we have observed that previous researchers worked on the SOFC/GT hybrid system. Few of them are related to direct hybrid system and few are related to indirect hybrid system. In few papers, power has been calculated from simulation and in few papers efficiency has been calculated. Also in few papers exergy have been calculated. Few have been using natural gases and in few biomass gasification is used.

In present thesis work, I have selected direct coupling SOFC/GT hybrid system with methane as a fuel. Coding has been done and simulation is performed. Simulation gives result of all major performance parameters such as Power, first law efficiency, second law efficiency, exergy destruction in all components, properties of substance at each state points. Also performance curves are drawn with varying parameters. All of these results are not available in a single literature using direct coupling hybrid system with methane as fuel.

# CHAPTER-3

## Modelling of Gas Turbine Power Plant

### 3.1 Introduction

Gas turbine power plant generates its power by the combustion of fuel in combustor, then using this fast flowing gas to drive gas turbine during expansion which gives power output. Gas turbine drives in similar way as high pressure steam drives a steam turbine. The main difference between gas turbine and steam turbine is that in the gas turbine there is an air compressor which is mounted on same shaft with the gas turbine. The air compressor draws fresh air and compresses it to a high pressure and then feed into combustion chamber and increases the burning flame intensity. As the gas turbine speed up, the air compressor also speeds up forcing more air into the combustion chamber which consequently increases the burning rate of fuel sending high pressure hot gases to the gas turbine and increasing its speed even more. To control the speed of turbine a fuel controller is installed on the fuel supply line which limits the fuel amount to the turbine. The gas turbine works on Brayton cycle. The efficiency of the cycle can be increased by increasing pressure ratio.

### 3.2 Components of gas turbine power plant

Gas turbine Power plant consists of mainly four components:

- (i) Compressor
- (ii) Combustion Chamber or Combustor
- (iii) Gas Turbine
- (iv) Heat exchanger



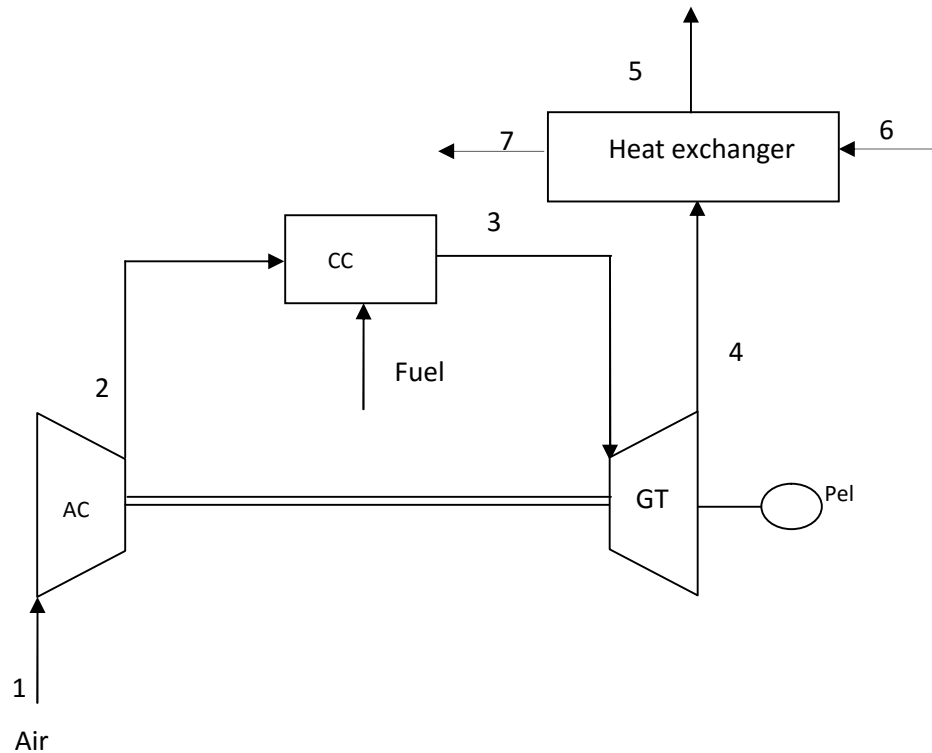


Figure 3.1 Schematic diagram of Gas turbine

### 3.2.1 Compressor Modelling:

Compressor draws working fluid (Usually air), pressurizes it and then feeds it to the combustion chamber. Following assumption are made to develop a mathematical model for the analysis of compressor:

- (a) Control volume approach
- (b) Steady state operation
- (c) Adiabatic operation of compressor
- (d) Kinetic and potential energy negligible
- (e) Air is mixture of Oxygen and Nitrogen so ideal gas mixture principle is valid.

Working principle of the compressor is to increase the pressure of the working fluid from the inlet state to the outlet state by compressing it. The outlet pressure can be calculated by using pressure ratio term. Pressure ratio is the ratio of outlet pressure to the inlet pressure.

$$P_r = P_2/P_1 \dots \dots \dots (3.1)$$

Where;

$P_r$  is the compression pressure ratio,  $p_1$  is the fluid pressure at the inlet of the compressor and  $P_2$  is the fluid pressure at the outlet of the compressor. If pressure ratio and inlet pressure is known, fluid pressure at the outlet of compressor can be determined by equation 3.1.

Work is required to be done on the compressor to compress the air. This specific work can be calculated by:

$$W_{com} = (h_2 - h_1) / \eta_{com, mech} \dots \dots \dots (3.2)$$

where;

$W_{com}$  is the specific work done on the compressor;  $h_1$  is the actual specific enthalpy of the fluid at the inlet of the compressor,  $h_2$  is the specific enthalpy of the fluid at the compressor outlet and  $\eta_{com, mech}$  is the mechanical efficiency of the compressor.

$h_1$  can be calculated by using the pressure and temperature at the compressor inlet and  $h_2$  can be calculated using the formula:

$$\eta_{com, isn} = (h_{2s} - h_1) / (h_2 - h_1) \dots \dots \dots (3.3)$$

where;

$\eta_{com, isn}$  is the isentropic efficiency of the compressor and  $h_{2s}$  is the specific enthalpy for isentropic compression. For an isentropic compression process of an ideal gas mixtures

$$s_{2s} - s_1 = X_{1N_2} [s_0(T_{2s}) - s_0(T_1) - R_u \ln(P_2/P_1)]_{N_2} + X_{1O_2} [s_0(T_{2s}) - s_0(T_1) - R_u \ln(P_2/P_1)]_{O_2} = 0 \dots \dots (3.4)$$

where;

$s_{2s}$  = specific entropy of the Air after isentropic compression,

$s_1$  = specific entropy of the Air at inlet of the compressor,

$T_1$  and  $T_{2s}$  = Temperature of the Air at inlet and outlet after isentropic compression,

$X_{1N_2}$  = mole fraction of the  $N_2$  in Air

$X_{1O_2}$  = mole fraction of the  $O_2$  in Air

$S_0$  = reference specific entropy (at 1.01325 bar and at corresponding temperature)

First of all evaluate the specific entropies of  $N_2$  and  $O_2$  at temperature  $T_1$ . Now by knowing molar fraction and specific entropies of  $N_2$  and  $O_2$ ,  $T_{2s}$  can be calculated from equation 3.4. After calculating  $T_{2s}$ , corresponding enthalpy of the mixture consisting  $O_2$  and  $N_2$  can be calculated.

Exergy destruction in compressor can be calculated by following equation:

$$E_d = W_{com} + (E_1 - E_2) \dots \dots \dots (3.5)$$

Where;

$E_d$ = exergy destruction in compressor,  $E_1$  and  $E_2$ = exergy of substance at inlet and outlet of compressor respectively,  $W_{com}$ = work input to the compressor

### 3.2.2 Combustion Chamber Modelling

Fuel enters into the combustion chamber and mixes with Air. The mixture of fuel and air burned and produces a high temperature and a high pressure gas streams that enters through the turbine section. Gas expands while passing through the Turbine section. A mathematical model is developed for analysis of combustion chamber. Following assumptions has been assumed.

- (a) Control Volume approach
- (b) Steady state reaction
- (c) Gas mixtures considered to be ideal
- (d) Kinetic and potential energy are negligible
- (e) Complete combustion
- (f) N<sub>2</sub> is inert
- (g) Heat transfer from the control volume is negligible

Fuel – Air Ratio = Molar flow rate of fuel / Molar flow rate of air

$$F/A \text{ Ratio} = \lambda = \dot{n}_F / \dot{n}_a \dots\dots\dots (3.6)$$

Where  $\dot{n}_F$  = Molar flow rate of fuel and  $\dot{n}_a$  = Molar flow rate of air

Applying first law of thermodynamic to the control volume:

$$\sum \dot{n}_i h_i + X_{fuel} LHV_{fuel} - \dot{W}_{cv} = \sum \dot{n}_e h_e \dots\dots\dots (3.7)$$

where;

$\dot{n}_i$  = Inlet molar flow rate,  $h_i$ = Inlet enthalpy,  $X_{fuel}$  = molar fraction at inlet,

$LHV_{fuel}$  = Lower heating value of fuel,  $\dot{W}_{CV}$  = Work transfer through the control volume

$\dot{n}_e$ =outlet molar flow rate,  $h_e$  = outlet enthalpy

Knowing the inlet enthalpy and LHV of fuel, outlet enthalpy can be calculated. By then outlet temperature can be evaluated through iteration.

Exergy destruction in combustion chamber can be calculated by following equation:

$$E_d = E_2 - E_3 \dots\dots\dots (3.8)$$

Where;  $E_d$ = exergy destruction in combustion chamber,  $E_1$  and  $E_2$ = exergy at the inlet and outlet of the combustion chamber respectively.

### 3.2.3 Gas Turbine Modeling

Hot combustion gas expands while passing through turbine section. Gas Turbine performs two functions. First, it drives the compressor for drawing pressurized air into the combustion chamber and secondly produces electric power through generator.

A mathematical model is developed for analysis of combustion chamber. Following assumptions had been assumed.

- (a) Control Volume approach
- (b) Steady state reaction
- (c) Gas mixtures at the gas turbine inlet is considered to be ideal
- (d) Kinetic and potential energy are negligible
- (e) Heat transfer from the control volume is negligible

While expanding through the turbine the pressure of the stream gets reduced. The pressure at the exit of the turbine can be calculated by using pressure ratio formula.

$$P_r = P_4/P_3 \dots\dots\dots (3.9)$$

Where;  $P_r$  = Pressure ratio of gas turbine,  $P_3$  and  $P_4$  = pressure at inlet and outlet of turbine

The specific work produced by the turbine is:

$$W_{tur} = (h_3-h_4)/\eta_{tur,mech} \dots\dots\dots (3.10)$$

$W_{tur}$  is the specific work done by the turbine;  $h_3$  is the actual specific enthalpy of the fluid at the inlet of the turbine which is same as the enthalpy at the outlet of combustion chamber,  $h_4$  is the specific enthalpy of the fluid at the turbine outlet and  $\eta_{tur,mech}$  is the mechanical efficiency of the turbine.  $h_4$  can be calculated using the formula:

$$\eta_{tur,isn} = (h_3-h_4) / (h_3-h_{4s}) \dots\dots\dots (3.11)$$

$\eta_{tur,isn}$  is the isentropic efficiency of the turbine and  $h_{4s}$  is the specific enthalpy for isentropic expansion. For an isentropic expansion process of an ideal –gas mixtures, entropy change is zero so;

$$S_{4s}(T_{4s},P_4) = s_3(T_3,P_3) \dots\dots\dots (3.12)$$

Where;

$s_{4s}$ =specific entropy of the Air after isentropic expansion,

$s_3$ = specific entropy of the Air at inlet of the turbine,

$T_3$  and  $T_{4s}$  = Temperature of the Air at inlet and outlet after isentropic expansion

Temperature  $T_{4s}$  can be calculated from equation 3.12. After calculating  $T_{4s}$ , enthalpy at  $T_{4s}$  can also be calculated.

Exergy destruction in turbine can be calculated by following equation:

$$E_d = E_3 - (E_4 + W_{tur}) \dots \dots \dots (3.13)$$

Where  $E_d$  = exergy destruction in gas turbine,  $E_3$  and  $E_4$  = exergy at the inlet and outlet of the gas turbine respectively and  $W_{tur}$  is the specific work done by the turbine.

### 3.2.4 Heat exchanger Modelling

Heat exchanger is a device in which heat is transferred from one moving fluid to another moving fluid.

Effectiveness of the heat exchanger can be given as:

$$\epsilon = (T_7 - T_6) / (T_4 - T_6) \dots \dots \dots (3.14)$$

Energy balance equation can be given as:

$$h_7 - h_6 = h_4 - h_5 \dots \dots \dots (3.15)$$

$T_6, T_7$  = temperature of cold stream at inlet and outlet respectively

$T_4, T_5$  = temperature of hot stream at inlet and outlet respectively

$h_4, h_5, h_6, h_7$  = enthalpy corresponding to  $T_4, T_5, T_6$  and  $T_7$  respectively.

Exergy destruction in heat exchanger can be calculated by following equation:

$$E_d = (E_4 + E_6) - (E_5 + E_7) \dots \dots \dots (3.16)$$

Where  $E_d$  = exergy destruction in gas turbine,  $E_4$  and  $E_6$  = exergy of cold and hot stream at heat exchanger inlet,  $E_5$  and  $E_7$  exergy of cold and hot stream at heat exchanger outlet.

# CHAPTER 4

## Modelling of Fuel Cell System

This chapter deals with the introduction of fuel cell, types of fuel cell, advantages, disadvantages, limitation and applications of various types of fuel cell, Solid oxide fuel cell and finally develop a mathematical model through the formulas.

### 4.1 Introduction of Fuel cell

Fuel cell is an electrochemical device. It directly converts chemical energy of fuel into electrical energy through an electrochemical reaction. Like a conventional cell it also has two porous electrodes and one electrolyte sandwiched between them. In a fuel cell fuel is continuously fed to the anode and oxidant (air or oxygen) is continuously fed to the cathode. Then an electrochemical reaction occurs in fuel cell which produces electricity and heat as main product and water as by product. Water is not a pollutant so fuel cell is a clean energy source. Heat is released during exothermic electrochemical reaction in the fuel cell. At anode, hydrogen splits into two parts by the help of catalyst; one is hydrogen ion and the second is electrons. These electrons flow from the anode to the cathode electrode through the external circuit to create a DC current. The electron in the end arrives at cathode electrode where these electrons recombined with hydrogen and oxidant. The hydrogen ions flow from anode to cathode through electrolyte. On reaching to the cathode these ions react with oxidant and produce heat and water.

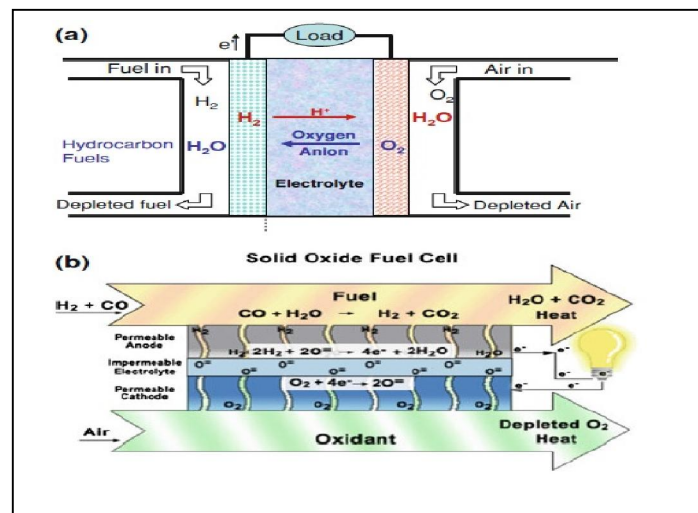
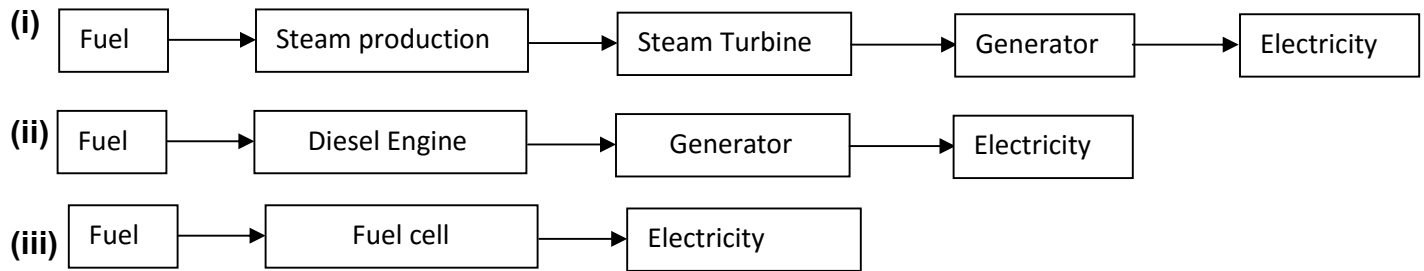


Figure 4.1 Fuel cell [32]

Generally chemical energy of fuels can be converted into electrical energy by following three methods. These are shown in Figure 4.2



**Figure 4.2 Methods of conversion of chemical energy into electrical energy**

In the first two processes electrical energy is obtained by converting chemical energy indirectly. In these 2 processes chemical energy of fuel firstly converted into heat energy then into mechanical energy and then finally into electricity. The process of conversion from heat energy into mechanical energy involves loss in energy so 100 % efficiency ca not be obtained whereas in third process whereas in the third process of converting chemical energy into electricity does not involve any heat loss so efficiency can reach to 100 %.

## 4.2 Types of fuel cells

Fuel cell can be classified in several ways:

- i) Based upon types of electrolyte
  - (a) Phosphoric acid fuel cell (PAFC)
  - (b) Alkaline fuel cell (AFC)
  - (c) Polymer electrolyte membrane fuel cell (PEMFC)
  - (d) Solid oxide fuel cell (SOFC)
  - (e) Molten carbonate fuel cell (MFC)
  
- ii) Based on types of fuel and oxidant
  - (a) Hydrogen – oxygen fuel cell
  - (b) Hydrogen rich gas – air fuel cell
  - (c) Hydrocarbon air fuel cell
  - (d) Synthetic gas- air fuel cell
  - (e) Ammonia – Air fuel cell

iii) Based upon operating temperature

- (a) Low temperature fuel cell
- (b) Medium temperature fuel cell
- (c) High temperature fuel cell
- (d) Very high temperature fuel cell

iv) Base on application

- (a) Fuel cell for commercial purpose
- (b) Fuel cell for submarine purpose
- (c) Fuel cell for defence purpose
- (d) Fuel cell for vehicle propulsion purpose
- (e) Fuel cell for space application

v) Based on chemical nature of electrolyte

- (a) Acidic electrolyte fuel cell
- (b) Alkaline electrolyte fuel cell
- (c) Neutral electrolyte fuel cell

The main classification is based upon the types of electrolyte. Each types of cell have its own characteristics, advantage and limitation which are tabulated in Table 4.1.

**Table 4.1 fuel cell Types, Description and Basic data [33-34]**

Fuel cell type	Electrolyte	Operating Temperature (°C)	Efficiency (%)	Charge carrier	Catalyst	Product water management	Advantages	Disadvantages	Most promising application
Alkaline fuel cell (AFC)	Solution of potassium hydroxide in water	60-70	36	OH <sup>-</sup>	Platinum	Evaporative	High efficiency. Low oxygen reduction reaction losses.	Must run on pure oxygen without CO <sub>2</sub> contamination	Space application with pure O <sub>2</sub> /H <sub>2</sub> available
Proton exchange membrane fuel cell (PEMFC)	Solid organic polymer poly-perfluorosulfonic acid	85-105	40	H <sup>+</sup>	Platinum	Evaporative	Low temperature operation, high efficiency, high H <sub>2</sub> power density, relatively rapid start-up	Expensive catalyst, durability of components not sufficient, poor quality waste heat, intolerance to CO, thermal and water management	Portable, automotive and stationery application



Phosphoric acid fuel cell (PAFC)	Solution of phosphoric acid in porous silicon carbide matrix	160-220	40-45	H <sup>+</sup>	Platinum	Evaporative	1-2% CO tolerant, good quality waste heat, demonstrated durability	Low power density, expensive, platinum catalyst used, slow start-up, loss of electrolyte	Premium stationery power
Molten carbonate fuel cell (MCFC)	Molten alkali metal carbonate in porous matrix	600-650	45-47	CO <sub>3</sub> <sup>2-</sup>	Nickel	gaseous	CO tolerant, fuel flexible, high quality waste heat, inexpensive catalyst	Electrolyte dissolves cathode catalyst, extremely long start-up time, CO <sub>2</sub> must be injected to cathode, electrolyte maintenance	Stationary power with cogeneration, continuous power application
Solid oxide fuel cell (SOFC)	Yttria(Y <sub>2</sub> O <sub>2</sub> ) stablized zirconia(ZrO <sub>2</sub> )	800-1000	48-55	O <sup>-</sup>	Perovskites	gaseous	CO tolerant, fuel flexible, high quality waste heat, inexpensive catalyst	Long start-up time, durability under thermal cycling, inactivity of electrolyte below 600°C	Stationary power with cogeneration, continuous power application

From Table 4.1, it is clear that Solid oxide fuel cell (SOFC) has high operating temperature (800-1000°C) and higher efficiency (48-55 %) in comparison to other fuel cells. Due to these reasons SOFC is preferred for Fuel cell and gas turbine hybrid system. Now we will discuss about Solid oxide fuel cell in detail.

### 4.3 Solid oxide fuel cell (SOFC)

Electricity generation from a solid oxide fuel cell is a very promising technology. Solid oxide fuel cell is a most advanced power production system with highest thermal efficiency in comparison to other power production plants. It has a fuel flexibility that means a wide variety of fuel can be used. A solid oxide fuel cell is an electrochemical cell which is required to be c fed continuously. In SOFC system ceramic materials are used as electrodes and electrolyte. The oxidation of fuel in SOFC is the main electrochemical reaction. A large range of material can be used in SOFC. A novel SOFC utilize solid oxide materials as an electrolyte. In SOFC Perovskites is being used as catalyst and Yttria (Y<sub>2</sub>O<sub>2</sub>) stablized zirconia (ZrO<sub>2</sub>) is being used as an electrolyte. SOFC has a higher power density so the compact design is feasible. An important advantage of SOFCs is the internal reforming

process. It is a process in which all fuels reformed and converted into hydrogen gas. This internal reforming reaction is an endothermic reaction. Heat for the process is available from electrochemical reaction. The reactions inside the cell (anode side) are as follows:



There is no water management problem in SOFC as it is a two phase gas-solid system. In other fuel cell system water management is a big challenger as there is a flooding of the catalyst layer or slow oxygen reaction kinetics. Different geometries of the SOFC is developed in past in which planer and tubular are most promising geometry.

#### **4.4 Types of Solid oxide fuel cell design**

Mainly 4 designs of SOFC are available (Figure 4.3) which are as follows:

1. Seal less tubular design
2. Planer design
3. Monolithic design
4. Segmented cell-in-series design

##### **1. Seal less Tubular design:**

This concept was pioneered by Westinghouse in 1980. The air is introduced through the centre of support tube and fuel passes through outside of this tube. There is no gas-tight-sealing problem as no sealing between cells are provided. In this type of system fuel cells in a bundle are arranged in series –parallel pattern. Individual cells can suffer catastrophic damage but stack does not need to go to offline, since the current is redistributed through other cells in parallel. That is why the system is more durable than other design. Some drawback of this type of design is that geometry is complex in nature, has limited method of fabrication, internal resistance and gas diffusion limitation.

##### **2. Planer design**

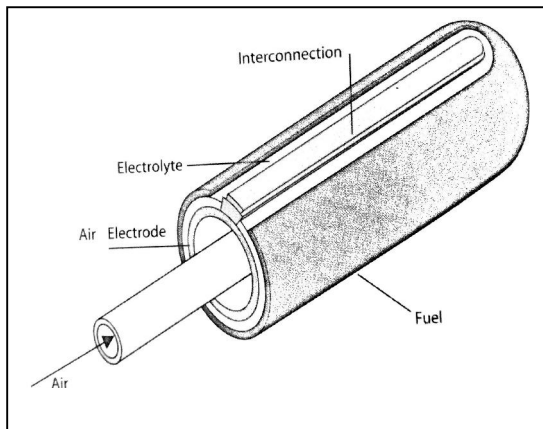
This design is simple to fabricate but suffers sealing problem. It can be Anode, cathode or electrolyte supported but mainly anode supported design is popular because the other design suffers excessive ionic and concentration losses. Integrity of this type of system is difficult to maintain for thermal variation for many start-ups and shut down.

### 3. Monolithic design

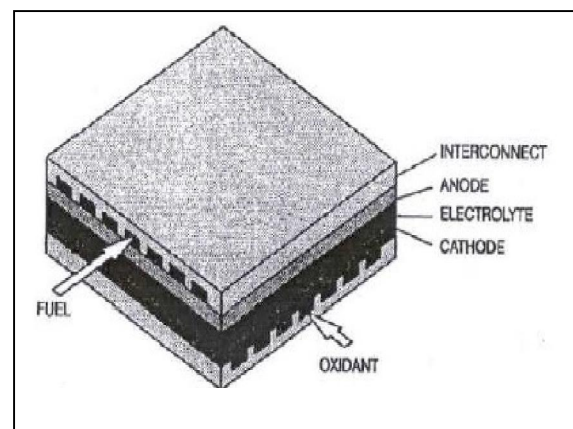
Monolithic design has the higher power density due to its high active area which is exposed per volume and there is short ionic paths through anode and cathode electrodes, electrolytes and interconnect which leads to a compact corrugated structure. The main problem of this design is the manufacturing of corrugated material. Cell cracking occurs if there is any difference in the thermal expansion.

### 4. Segmented cell-in-series design

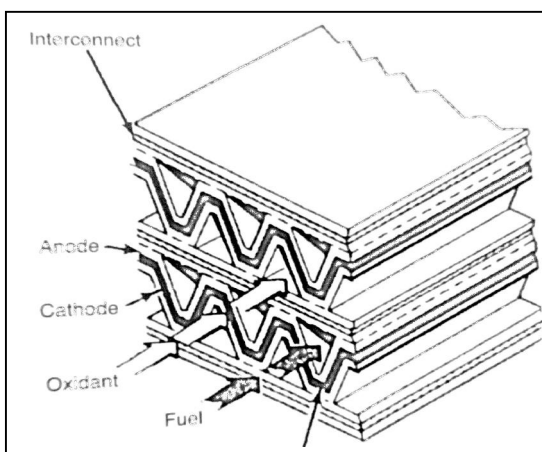
The design of this system is similar to seal less Tubular design with the difference that fuel enters through the centre of support tube and oxidant passes through outside of the tube.



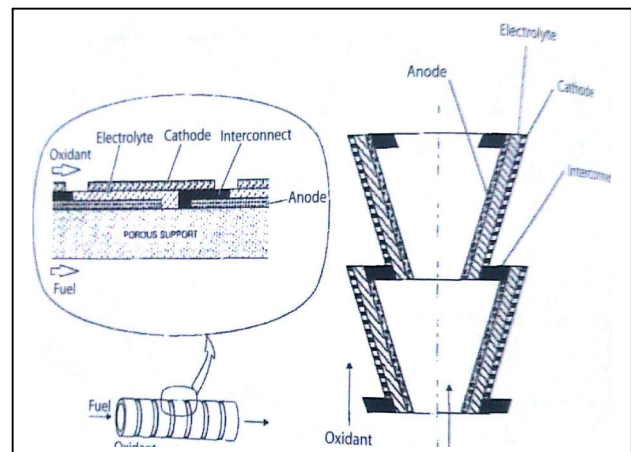
(a) Seal-less tubular design [33]



(b) Planer cell design [15]



(c) Monolithic cell design[33]



(d) Segmented cell-in-series design[33]

**Figure 4.3**

## 4.5 Electrochemical reaction

The electrochemical reaction is somewhat similar to chemical reaction. In electrochemical reaction overall global reaction and thus the chemical energy difference between beginning and end states of reactant and product are identical to the analogous chemical reaction. However, an electrochemical reaction circulates current through a continuous circuit to complete the reaction, while a pure chemical reaction does not complete the cycle. In figure 4.4 a schematic of electrochemical reaction is shown. The electrochemical reaction for fuels such as methane is as follows:

➤ Reaction when Methane is used as a fuel:

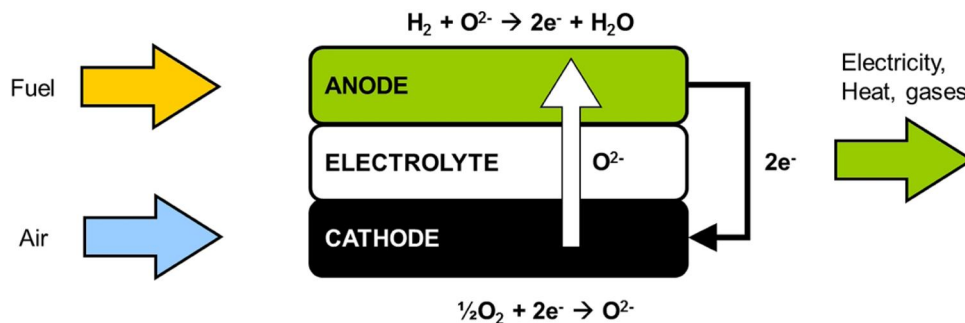
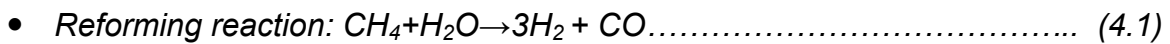


**Figure 4.4: Electrochemical reaction in fuel cell [35]**

## 4.6 Stacking of Fuel cell

In a fuel cell, desired cell power output and cell current can be obtained by:

- Increasing the total active surface area of the electrodes
- Increasing molar flow rate of reactants
- By utilising both of the above combination.

However, the single cell output voltage has limitation of fundamental electrochemical potential related to reacting species involved. Its value is less than one volt (<1 V) for the

real operating condition. To achieve a compact design and higher voltage, several individual cells are connected in series to form a stack. For the stack in which cells are connected in series, total stack current is proportional to electrodes surface area of individual cell in stack and is same for all cells. The operating cell voltage is sum of individual cells. If the cells are connected parallel then voltage for each cell is same and total current is the sum of individual cell.

$$N_{\text{stack}} = N_{\text{cell}} / N_{\text{cell}}^{\text{stack}} \dots\dots\dots (4.6)$$

$$N_{\text{cell}} = A_t / A_c \dots\dots\dots (4.7)$$

$$A_t = I / J \dots\dots\dots (4.8)$$

$$V_{\text{stack}} = N_{\text{cell}}^{\text{stack}} \times V_{\text{cell}} \dots\dots\dots (4.9)$$

Where;

$N_{\text{cell}}$  = total no. of cell,  $N_{\text{cell}}^{\text{stack}}$  = no. of cell in each stack,  $N_{\text{stack}}$  = No. of stack

$A_t$  = total active surface area,  $A_c$  = surface area of one cell,  $J$  = Current density,

$I$  = Total current,  $V_{\text{cell}}$  = Cell operating voltage

### 4.7 Faraday’s Law for fuel cell

Faraday’s law govern the production and consumption of electrolysis process in an electrochemical reaction. According to faraday’s law:

1. For the specific charged passed, mass of the total products are in proportion to electrochemical equivalent weights of the total products.
2. The products formed are directly proportional to charge released. Also the reactants consumed are directly proportional to charge released.

The 2<sup>nd</sup> law is most important for study of fuel cell. The current produced is proportional to either mass reacted or produced. In a pure electrochemical reaction molar flow rate of consumption or production is given as follows:

$$n_x = (JA_t) / n_e F = I / n_e F \dots\dots\dots (4.10)$$

Where;  $J$  = current density,  $A_t$  = total active surface cell area,  $n$  = no. of electron released,  $F$  = faraday’s constant

## 4.8 Efficiency related terms

### (a) **Faradic efficiency:**

It is defined as measure of percent utilization of reactants in a galvanic process

$$\epsilon_f = \text{theoretical required rate of reactant} / \text{Actual rate of reactant supplied...} \quad (4.11)$$

### (b) **Fuel utilization efficiency:**

The faradic efficiency is known as Fuel utilization efficiency when it is used for fuel in a galvanic redox reaction. It is defined as the ratio of theoretically required rate of fuel to the actual rate of fuel supplied. It is a very important parameter in the fuel cell reaction. When the fuel utilization factor is very high it has an advantage that almost all hydrogen which is produced by the internal reforming reactions is consumed within the fuel cell during the electrochemical reaction. Thus, fuel cell produces more electricity.

$$U_f = \text{theoretically required rate of fuel} / \text{Actual rate of fuel supplied.....} \quad (4.12)$$

### (c) **Air utilization efficiency:**

Air utilization efficiency is defined as the ratio of theoretically required rate of air to the actual rate of air supplied

$$U_a = \text{theoretically required rate of air/actual rate of air supplied.....} \quad (4.13)$$

(d) **Current efficiency:** In electrolyte reaction some side reaction takes place due to which some insufficiency may occur and so less than a complete conversion. The current efficiency is defined as the ratio of actual required rate of species reacted or produced to the theoretically rate of species reacted or produced

$$\epsilon_c = \text{Actual required rate of species reacted or produced} / \text{theoretically rate of species reacted or produced.....} \quad (4.14)$$

### (e) **Cathodic Stoichiometry:**

$$\lambda_c = \text{Actual rate of oxidizer delivered to cathode/theoretically rate of oxidizer required.....} \quad (4.15)$$

$$= 1 / \text{cathodic faradic efficiency.....} \quad (4.16)$$

**(f) Anodic Stoichiometry:**

$$\lambda_a = \text{Actual rate of fuel delivered to anode / theoretically rate of fuel required....} \quad (4.17)$$
$$= 1/ \text{anodic faradic efficiency.....} \quad (4.18)$$

**(g) Molar flow rate of reactant at entry of fuel cell**

$$\dot{n}_{in} = (\lambda \times I)/(n_e \times F) \dots\dots\dots (4.19)$$

**(h) Molar flow rate of consumption of reactant in fuel cell**

$$\dot{n}_c = I / (n_e \times F) \dots\dots\dots (4.20)$$

**(i) Molar flow rate of reactant at the exit of fuel cell**

$$\dot{n}_{out} = \dot{n}_{in} - \dot{n}_c = (\lambda - 1) \times I / (n_e \times F) \dots\dots\dots (4.21)$$

where;  $\lambda$  = Stoichiometry ratio,  $I$  = total current produced

## 4.9 Cell voltage related terms

**(1) Maximum expected voltage( $E_0$ )**

This is the theoretical maximum voltage which could be reached in a fuel cell or we can say this is the maximum possible voltage without considering irreversible polarization losses. We will discuss about the polarization curve in coming section of the chapter. Now we will derive the expression of this voltage as follows:

For a compressible system,

$$dU = \delta Q - \delta W \dots\dots\dots (4.22)$$

For a reversible system,

$$\delta Q = TdS \dots\dots\dots (4.23)$$

$$\delta W = \text{Mechanical work} + \text{electrical work} = \delta W_{mech} + \delta W_e = PdV + \delta W_e \dots\dots\dots (4.24)$$

From equation (4.22), (4.23) and (4.24),

$$dU = TdS - PdV - \delta W_e \dots\dots\dots (4.25)$$

For constant temperature process, change in Gibbs free energy,

$$dG = dH - TdS \dots\dots\dots (4.26)$$

For constant pressure process change in enthalpy,

$$dH = dU + PdV \dots\dots\dots (4.27)$$

Putting value of  $dU$  from equation (4.25) into equation (4.27) we get,

$$dH = TdS - \delta W_e \dots\dots\dots (4.28)$$

Putting value of  $dH$  from equation (4.28) into equation (4.26) we get,

$$dG = - \delta W_e \dots\dots\dots (4.29)$$

This is the maximum electrical work that can be obtained from the system for reversible process. It can also be represented by the electrical work required to move a given charge,

$$W_e = n_e F E_0 \dots\dots\dots (4.30)$$

From equation (4.29) and (4.30),

$$E_0 = \Delta G/n_e F \dots\dots\dots (4.31)$$

**(2) Thermal voltage( $E_{00}$ )**

Thermal voltage is the maximum voltage which can be obtained in a reversible adiabatic system.

For a reversible adiabatic process, change in entropy is zero so from equation (4.28):

$$dH = dG \dots\dots\dots (4.32)$$

So we can show that;

$$E_{00} = -\Delta H/n_e F \dots\dots\dots (4.33)$$

**(3) Maximum possible thermodynamic efficiency**

It is the ratio of maximum expected voltage to the thermal voltage

$$\eta_{th,max} = E_0/ E_{00} = \{-\Delta G/(n_e \times F)\} / \{-\Delta H/(n_e \times F)\}$$

$$\text{From equation 4.26, } \eta_{th,max} = (\Delta H - T\Delta S)/ \Delta H = 1 - T\Delta S/ \Delta H \dots\dots\dots (4.34)$$

**4.10 Nernst Voltage**

It is the maximum expected open circuit voltage in a fuel cell. From equation (4.28) and (4.29) it is clear that, Thermal voltage depends only upon the temperature whereas maximum expected voltage depends upon both temperature and pressure of the reactant and product. Nernst equation gives the expression of maximum expected voltage as a function of temperature and pressure and also gives the expression of an established thermodynamic equilibrium.

Expression for Nernst voltage is given as following:

Considering an electrochemical reaction in a fuel cell:



where;



$v_A$  and  $v_B$ ,  $v_C$  and  $v_D$  are the stoichiometry coefficient of the reactants and products in a balanced electrochemical reaction respectively.

From thermodynamics of systems in equilibrium:

$$\Delta G = \Delta G(T) - R_u T \ln [(a_A^{v_A} a_B^{v_B}) / (a_C^{v_C} a_D^{v_D})] \dots \dots \dots (4.36)$$

Where; the  $a_A$  and  $a_B$ ,  $a_C$  and  $a_D$  are the thermodynamic activity coefficient of the reactants and products in a balanced electrochemical reaction respectively.

To convert above equation in voltage form, dividing by  $nF$ :

$$E(T,P) = E = [\Delta G(T)/n_e F] - (R_u T/n_e F) \times \ln [(a_A^{v_A} a_B^{v_B}) / (a_C^{v_C} a_D^{v_D})] \dots \dots \dots (4.37)$$

This equation is known as General Nernst voltage expression. The Nernst voltage expression for hydrogen and methane fuel cell can be given by using equation (4.37):

Nernst equation for methane fuel cell:

$$E = E_0 + (R_u T/8F) \ln [(P_{CH_4} P_{O_2}^2) / (P_{H_2O}^2 P_{CO_2})] \dots \dots \dots (4.38)$$

Nernst equation for Hydrogen fuel cell:

$$E = E_0 + (R_u T/2F) \ln [(P_{H_2} P_{O_2}^{1/2}) / (P_{H_2O})] \dots \dots \dots (4.39)$$

## 4.11 Losses in terms of voltage in a fuel cell

There are five types of voltage losses which are also called as overpotential loss or polarization loss occurs in a fuel cell due to which actual cell voltage is lesser than maximum expected voltage. These are as follows:

- (1) Activation Loss
- (2) Ohmic Loss
- (3) Concentration loss
- (4) Losses due to crossover of species and internal current
- (5) Losses due to change in entropy

### 4.11.1 Activation loss:

In an electrochemical reaction, if the probability of the energy related to molecules is low then activation energy must be supplied in terms of voltage to initiate and increase the speed of reaction. This supplied energy is called as an activation loss. It dominates at low current densities. In Solid oxide fuel cell this loss is less dominant as the operating temperature is high. Activation loss in fuel cell is somewhat similar to ignition energy which is provided in a combustion chamber having gasoline vapour and air to enable the

spontaneous reaction to proceed. It is evaluated by using Butler-volume model of kinetics. The Butler volume equation is given as:

$$J = i_o (C_s/C^*)^\gamma [\exp(\alpha_a F \eta / R_u T) - \exp(-\alpha_c F \eta / R_u T)] \dots\dots\dots (4.40)$$

where;

J= total current density

$i_o$ = exchange current density of the electrode

$C_s$ =electrode concentration of the reactant at the surface of the catalyst surface

$C^*$  = reference concentration of the reactant at STP condition

$\gamma$  = reaction order for elementary charge transfer step, which can vary for different electrodes and reactant and is determined experimentally.

$\alpha_a F \eta / R_u T$ = oxidation reaction at the particular electrode

$\alpha_c F \eta / R_u T$ = reduction reaction at the particular electrode

$\alpha_a$ = anodic charge transfer coefficient

$\alpha_c$  = cathodic charge transfer coefficient

$\eta$ = Activation loss

The butler volume equation can also be expressed as:

$$J = i_{oa} \times [\exp\{(\alpha_a n_e x F \eta_{aano}) / (R_u x T)\} - \exp\{-(1 - \alpha_a) n_e x F \eta_{aano} / (R_u x T)\}] \dots\dots\dots (4.41)$$

$$J = i_{oc} \times [\exp\{(\alpha_c n_e x F \eta_{acat}) / (R_u x T)\} - \exp\{-(1 - \alpha_c) n_e x F \eta_{acat} / (R_u x T)\}] \dots\dots\dots (4.42)$$

$$i_{oa} = k_a \times (P_{H_2}/P_0) \times (P_{H_2O}/P_0) \times \exp [-E_a / (R_u \times T)] \dots\dots\dots (4.43)$$

$$i_{oc} = k_c \times (P_{O_2}/P_0)^m \times \exp[-E_c / (R_u \times T)] \dots\dots\dots (4.44)$$

where;

$i_{oa}$  and  $i_{oc}$  = exchange current density for anode and cathode respectively

J= Total current density

$n_e$  = No. of electrons released

$E_a$  and  $E_c$  = Activation energy for anode and cathode respectively

$\eta_{aano}$  and  $\eta_{acat}$  = Activation loss for anode and cathode electrodes respectively

$P_{H_2}$  = partial pressure of Hydrogen

$P_{H_2O}$  = Partial pressure of Water

$P_{O_2}$  = partial pressure of Oxygen

$P_0$ = Reference pressure

$k_a$  and  $k_c$  =Pre-exponential factor for anode and cathode respectively

m=Slope

#### 4.11.2 Ohmic loss:

Ohmic loss occurs due to Ohmic resistance in various components of the fuel cell such as in anode electrode, cathode electrode, electrolyte, and interconnection between mating parts.

The ohmic loss is evaluated by using ohm's law:

$$\eta_{ohm} = i \times A (\sum r_k) \dots \dots \dots (4.45)$$

The total ohmic loss in a fuel cell can be written as:

$$\eta_{ohm} = i \times R_{ohm} = i \times (R_{anode} + R_{cathode} + R_{electrolyte} + R_{interconnections}) \dots \dots \dots (4.46)$$

$R_{ohm}$  is calculated by using:

$$R_{ohm} = \rho \delta / A \dots \dots \dots (4.47)$$

where;

$R_{ohm}$  = Ohmic resistance ( $\Omega$ )

$\rho$  = resistivity ( $\Omega$ -m)

$\delta$  = linear path length of ion travel (m)

A = cross-sectional area of ion travel ( $m^2$ )

Resistivity can be calculated as follows:

$$\rho = a \times \exp (b/T) \dots \dots \dots (4.48)$$

where; a and b is constant, T is fuel cell operating temperature.

Value of constant a and b for various components depends upon the materials. The value of constants for tubular SOFC of particularly following material is given [36] in Table A.1 in Appendix A. (a) Cathode tube of lanthanum manganite, (b) Electrolyte of Ytria stabilized zirconia (YSZ), (c) Anode electrode of Ni/YSZ (d) Interconnection of doped lanthanum chromite.

#### 4.11.3 Concentration Loss:

According to Nernst equation (4.39), voltage drops if there is reduction of fuel and air partial pressures occurs. Fuel which is supplied to the anode electrode is used continuously by the electrochemical reaction, resulting into a local reduction in partial pressure of fuel. If the fuel is not replenished readily then the partial pressure could decrease dramatically. Also due to fluid resistance the fuel outlet pressure is smaller than inlet causing pressure drop. Similarly reduction in air partial pressure occurs at cathode electrode. According to Nernst equation,

the concentration loss is determined by the difference between actual Nernst voltage and open circuit Nernst voltage:

Total concentration loss= Concentration loss at anode + Concentration loss at cathode

$$\eta_c = \eta_{c\text{ano}} + \eta_{c\text{cat}} = (R_u T / n_e F) \ln [1 - J/i_{L\text{a}}] + (R_u T / n_e F) \ln [1 - J/i_{L\text{c}}] \dots \dots \dots (4.49)$$

Each electrode has a separate limiting current density and the concentration loss. For hydrogen fuel anode concentration loss is negligible due to high concentration and mass diffusivity of hydrogen. So for hydrogen fuel equation (4.49) becomes:

$$\eta_c = (R_u T / n_e F) \ln [1 - J/i_L] \dots \dots \dots (4.50)$$

where,

$i_L$  = Limiting current density which is evaluated as follows:

For a one dimensional transport to the catalyst surface,

$$i_L A / n_e F = - D_j A (dC_j / dx) + C_j A v_x \dots \dots \dots (4.51)$$

In equation (4.51), First term represent consumption, second is Diffusion transport and the third term represent Advective transport.

If we assume zero bulk flow velocity in a one dimensional flux to the electrode surface in x direction, the equation (4.51) becomes:

$$i_L = -n_e F D_{\text{eff}} (C_\infty - C_s) / \delta \dots \dots \dots (4.52)$$

At limiting condition  $C_s$  becomes zero so the equation (4.52) becomes

$$i_L = -n_e F D_{\text{eff}} C_\infty / \delta \dots \dots \dots (4.53)$$

where;

$$D_{\text{eff}} = \text{Knudsen Effective Diffusion coefficient} = D_{K,i(\text{eff})} = D_{K,i} \times \epsilon / \xi \dots \dots \dots (4.54)$$

$$D_{K,i} = \text{Knudsen Diffusion coefficient} = 97 \times r \times [T_{\text{cell}} / M_i]^{0.5} \dots \dots \dots (4.55)$$

$$C_\infty = \text{reactant concentration at the boundary with the flow channel} = y_i P / R_u T \dots \dots (4.56)$$

Where;

Subscript i represents gaseous components (such as H<sub>2</sub>O, H<sub>2</sub>, O<sub>2</sub> or N<sub>2</sub>),

r = electrode pore radius (m), T<sub>cell</sub> = cell operating temperature (K),

M<sub>i</sub> = molecular weight (kg/kmol) of gaseous components,

δ = Diffusion layer thickness,

ε = porosity,

ξ = tortuosity

The binary gas phase diffusion coefficients for both anode electrode and cathode electrode on the basis of molecular volume are as follows:

$$D_{ik} = \left[ \left\{ 10^{-3} \times T^{1.75} \times \left( \frac{1}{M_i} + \frac{1}{M_k} \right) \right\} / \left\{ P \times \left( v_i^{0.33} + v_k^{0.33} \right)^2 \right\} \right] \dots \dots \dots (4.57)$$

Where;

i and k represents gaseous components which makes the binary gas mixture

(a) H<sub>2</sub>-H<sub>2</sub>O at anode and (b) O<sub>2</sub>-N<sub>2</sub> at cathode, v= fuller diffusion volume given in table A.2 of appendix A.

The overall value of effective diffusion coefficient can be calculated for each gas as follows:

$$1/D_{i(\text{eff})} = 1/D_{ik(\text{eff})} + 1/D_{ki(\text{eff})} \dots \dots \dots (4.58)$$

The effective coefficient for anode is given as:

$$D_{An(\text{eff})} = P_{H_2O}/P \times D_{H_2(\text{eff})} + P_{H_2}/P \times D_{H_2O(\text{eff})} \dots \dots \dots (4.59)$$

Where; P<sub>H<sub>2</sub>O</sub> and P<sub>H<sub>2</sub></sub> is partial pressure of H<sub>2</sub>O and H<sub>2</sub> respectively, P is total pressure

The effective coefficient for cathode is given as:

$$D_{cat(\text{eff})} = D_{O_2(\text{eff})} \dots \dots \dots (4.60)$$

**4.11.4 Fuel crossover and internal currents related loss**

Fuel crossover is an incident that occurs when a definite amount of fuel diffuse from anode to cathode via electrolytes without reacting electrochemically. In the fuel cell, at the cathode electrode it directly reacts with oxygen and producing heat. Moreover; the real electrolyte is generally a good ionic conductor, could also support electron conduction which determine the internal currents. Both of phenomena determine voltage loss. In first case, a quantity of fuel is combusted. In second case, external electrical load cannot use electrons. These two are summarized as a single loss which is called as ‘mixed potential’ introducing the term of internal current density. This type of loss is generally neglected in SOFC.

**4.11.5 Losses related to change in entropy**

This type of loss is developed due to change in entropy of reactant in an electrochemical reaction.

## 4.12 Polarization Curve

Polarization curve is a fuel cell characterizing curve which evaluates the fuel cell performance. It is a plot between cell voltage and current density. Figure 4.5 is a typical polarization curve for Hydrogen-Air fuel cell with negative entropy of reaction. From figure 4.5, five loss regions are shown which are as follows:

Region I: Dominated by Activation loss

Region II: Dominated by Ohmic loss

Region III: Dominated by Concentration loss

Region IV: Dominated by loss due to species crossover

Region V: Dominated by loss due to Entropy change

A polarization curve between cell voltage and current density of Solid oxide fuel cell is shown in Figure 4.6. The graph shows in Figure 4.6 is plotted to evaluate Ohmic polarization or Ohmic loss at various cell operating temperature.

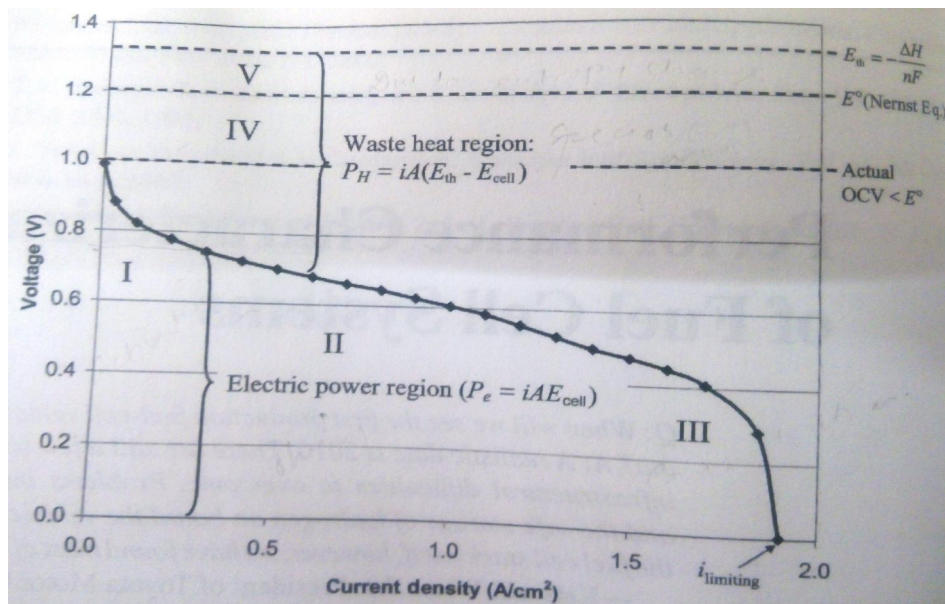


Figure 4.5 Typical polarization curves for fuel cell with significant kinetics, Ohmic, concentration and crossover [41]

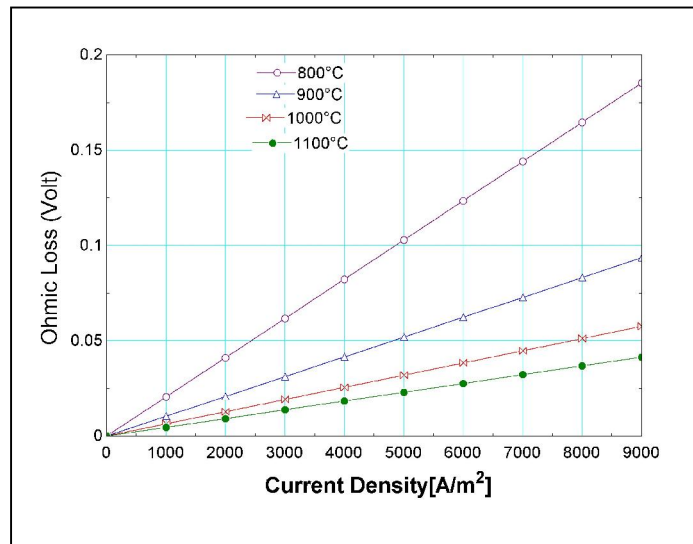


Figure 4.6 Variation of Ohmic loss with current density in SOFC

### 4.13 Cell Power output

$$\text{Cell power Output } P = V_{\text{cell}} \times I \dots\dots\dots (4.61)$$

Where; P= Total Cell DC Power Output,  $V_{\text{cell}}$ = actual cell voltage

I= Total cell current

$$\text{Cell AC power output } P_{\text{AC}} = P \times \text{Inverter efficiency} \dots\dots\dots (4.62)$$

### 4.14 Exergy analysis of Fuel cell

Total exergy is the sum of physical exergy, chemical exergy, potential exergy and kinetic exergy.

$$EX = EX_{\text{ph}} + EX_{\text{ch}} + EX_{\text{K}} + EX_{\text{p}} \dots\dots\dots (4.63)$$

If the change in kinetic and gravitational potential is neglected then equation becomes

$$EX = EX_{\text{ph}} + EX_{\text{ch}} \dots\dots\dots (4.64)$$

**Physical exergy** is the maximum amount of work that can be obtained by making a stream of matter from its initial state to the environmental state with the exchange of heat only with the thermal reservoir of the environment.

$$\text{Physical exergy} = EX_{\text{ph}} = (h-h_0) - T_0(S-S_0) \dots\dots\dots (4.65)$$

Physical exergy at anode inlet:

$$EX_{\text{ph,a,in}} = h_{\text{ano,in}} - h_{0,\text{ano,in}} - T_0(S_{\text{ano,in}} - S_{0,\text{ano,in}}) \dots\dots\dots (4.66)$$

Physical exergy at Cathode inlet:

$$Ex_{ph,c,in} = h_{cat,in} - h_{0,cat,in} - T_0(S_{cat,in} - S_{0,cat,in}) \dots \dots \dots (4.67)$$

Physical exergy at anode inlet:

$$Ex_{ph,a,out} = h_{ano,out} - h_{0,ano,out} - T_0(S_{ano,out} - S_{0,ano,out}) \dots \dots \dots (4.68)$$

Physical exergy at Cathode inlet:

$$Ex_{ph,c,out} = h_{cat,out} - h_{0,cat,out} - T_0(S_{cat,out} - S_{0,cat,out}) \dots \dots \dots (4.69)$$

**Chemical exergy** is the maximum amount of work that can be obtained by making a stream of matter from environment state to the total dead (unrestricted) state with the exchange of heat and exchange of substances only with the environment.

$$Ex_{ch} = R_u T_0 \sum x_i \ln x_i + \sum x_i ex_{ch,i}^0 \dots \dots \dots (4.70)$$

Where,

$x_i$  = mole fraction of the  $i^{th}$  species in the flow

$Ex_{ch,i}^0$  = molar chemical exergy of the  $i^{th}$  species at reference

Exergy balance for fuel cell is given as:

$$Ex_{ph,a,in} + Ex_{ph,c,in} + Ex_{ch,a,in} + Ex_{ch,c,in} = Ex_{ph,a,out} + Ex_{ph,c,out} + Ex_{ch,a,out} + Ex_{ch,c,out} + Ex_d + V_{cell} I \dots \dots \dots (4.71)$$

$Ex_{ph,a,in}$  and  $Ex_{ph,c,in}$  = physical exergy at anode and cathode

$Ex_{ch,a,in}$  and  $Ex_{ch,c,out}$  = chemical exergy at anode and cathode

$h_{ano,in}$  and  $h_{cat,in}$  = enthalpy of substance at anode and cathode inlet respectively

$h_{ano,out}$  and  $h_{cat,out}$  = enthalpy of substance at anode and cathode outlet respectively

$h_{0,ano,in}$  and  $h_{0,cat,in}$  = enthalpy of substance at reference condition to anode and cathode inlet respectively

$h_{0,ano,out}$  and  $h_{0,cat,out}$  = enthalpy of substance at reference condition to anode and cathode outlet respectively

$S_{ano,in}$  and  $S_{cat,in}$  = entropy of substance at anode and cathode inlet respectively

$S_{ano,out}$  and  $S_{cat,out}$  = entropy of substance at anode and cathode outlet respectively

$S_{0,ano,in}$  and  $S_{0,cat,in}$  = entropy of substance at reference condition to anode and cathode inlet respectively

$S_{0,ano,out}$  and  $S_{0,cat,out}$  = entropy of substance at reference condition to anode and cathode outlet respectively

$Ex_d$  = exergy destruction



#### **4.15 Environmental Impact of SOFC:**

In general environmental impact of SOFC depends upon the type of fuel used in the system. If the fuel is rich in hydrogen or pure hydrogen is used then there is almost zero emission other than water and heat. But there is lots of problem in storage and transportation of hydrogen. Higher efficiency of SOFC leads to lesser use of fuel to produce a required amount of electricity which consequently results into a lower emission of CO<sub>2</sub> which is the main greenhouse gas accountable for global warming. If the hydrogen is extracted from natural gas through reformation processes then SOFC have no net emission of CO<sub>2</sub> because any carbon released in the process will be taken from the atmosphere by photo-synthesis process of plants. Also there is very low (near zero) level of other pollutants such as NO<sub>x</sub> and SO<sub>x</sub> and particulates from SOFC system and therefore it eliminates 20000 of kgs of acid rain and smog causing pollutant from the atmosphere. Ultimately the SOFC gives lowest emission in comparison to other conventional power plant system. SOFC provides high quality heat which can be used in refrigeration and air conditioner without harming g the environment.

# CHAPTER 5

## Modelling of SOFC/GT Hybrid system

### 5.1 Introduction

The Hybrid systems are the system in which a gas turbine is coupled with a fuel cell to generate power. Fuel cell will act as non-heat engine and the gas turbine will act as heat engine. This coupled system provides a far better efficiency than produced by a single system. As fuel cell is a clean energy source the hybrid system has a very low level of pollution. The efficiency achieved in this hybrid system is comparable with the other large power plants. Hybrid system is the combination of gas turbine and fuel cell to achieve a higher efficiency around 60-70%. The fuel cell generates the major portion of the plant power output and the gas turbine generates a fraction of total power output. The micro gas turbine has advantage of low weight and volume but also has lower efficiency of about 30% and more emissions in comparison to other normal gas turbine. A Solid oxide fuel cell has a high efficiency with low emission. The cell operating temperature is very high which gives high temperature of exhaust stream that can be utilised by coupling the turbine at cell outlet. This high temperature stream expands in turbine producing power and the turbine exhaust stream still have a sufficient heat which can be utilised further to heat the fuel and air before entering into anode and cathode respectively. The fuel utilization efficiency of solid oxide fuel cell is 80-85% therefore; there is possibility of combustion of fuel cell exhaust stream into the combustor of turbine to further enhance the efficiency of the system.

### 5.2 Hybrid system types

The hybrid system can be classified on the basis of coupling method. These are as follows:

1. Indirect Integration
2. Direct Integration

Each types of system have its own advantages and limitation. Application areas may also be different now we will discuss each types of hybrid system in details.

### 5.2.1 Indirect Integration:

Indirect integration is also called integration of fuel cell with gas turbine via heat exchanger. A heat exchanger is used in place of the combustor of gas turbine. Air which comes from the air compressor gets heated in this heat exchanger by the exhaust stream of fuel cell. Anode and cathode gases are preheated with gas turbine exhaust stream. In the indirect hybrid system, Solid oxide fuel cell can operate at atmospheric conditions. The advantage of this type of system is that it reduces the requirement of sealant in the fuel cell stack but heat exchanger suffers the problem of operating at very high and pressure temperatures differences. The heat exchanger requires special material for operating at such a high temperature and pressure. The high temperature alloys, ceramic material or some other expensive material can be used and hence, generally this system is not used so much. Development of heat resistant and inexpensive material is required to enhance the life span of such system. There is also an interconnection problem between fuel cell and heat exchanger.

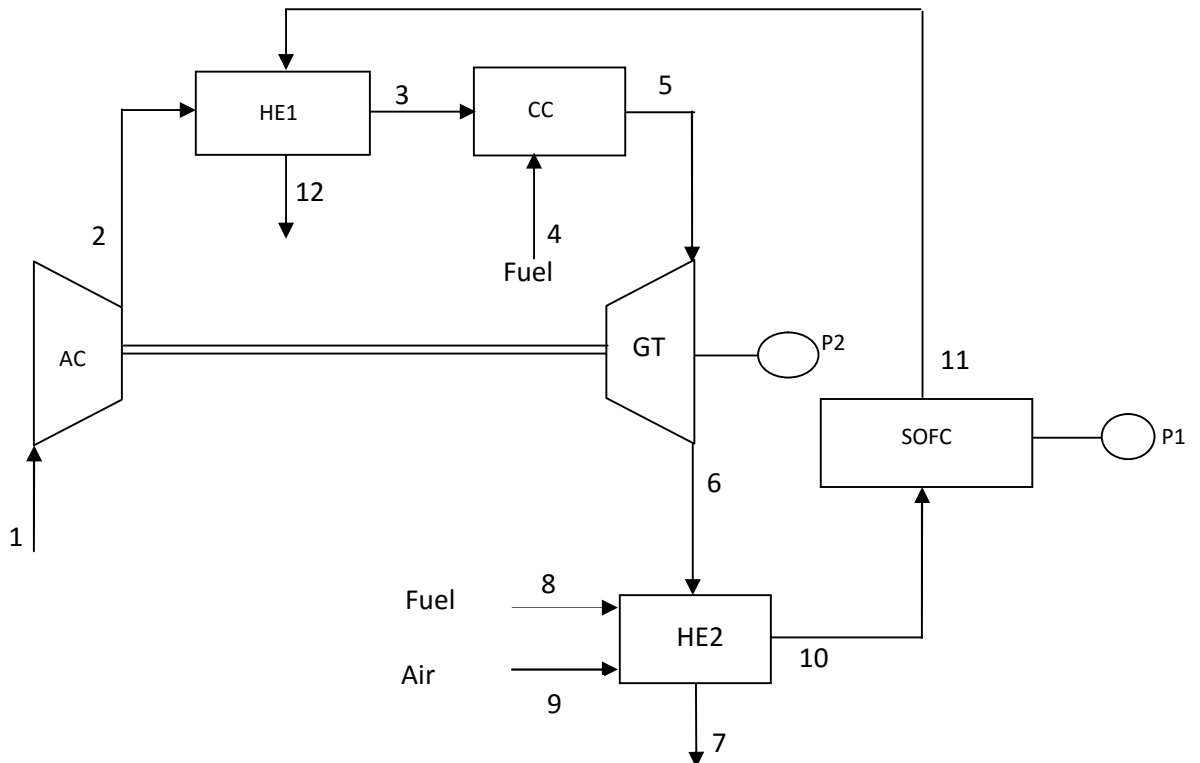


Figure 5.1 Flow Diagram of Indirect Integration hybrid systems

**Table 5.1.State points and abbreviation for indirect integration hybrid system**

AC	Air Compressor
HE1	Heat exchanger 1
HE2	Heat exchanger 2
SOFC	Solid oxide fuel cell
CC	Combustion Chamber
GT	Gas turbine
P1	Electrical power output from SOFC
P2	Electrical power output from gas turbine
State 1	Inlet to air compressor
State 2	Outlet from air compressor and inlet to Heat exchanger 1
State 3	Air leaving the heat exchanger 1 and entering into CC
State 4	Fuel supply into combustion to achieve the desired gas turbine inlet temperature
State 5	Mixture of gases leaving HE1 and entering into GT
State 6	Mixture of gases leaving GT and entering into HE2
State 7	Mixture of gases leaving HE2 and entering into atmosphere
State 8	Fuel entering into HE2 at atmospheric condition
State 9	Air entering into HE2 at atmospheric condition
State 10	gases leaving HE2 and entering into SOFC
State 11	Mixture of gases leaving SOFC and entering into heat exchanger 1
State 12	Mixture of gases leaving heat exchanger 1 and entering into atmosphere

### **5.2.2 Direct Integration**

Direct integration is also called direct fuel cell cycle. In this type of hybrid system the fuel cell is directly coupled with the gas turbine by replacing the combustor of the gas turbine. The direct integration hybrid system is more accepted than indirect system. Indirect system works at atmospheric condition whereas direct system can operate at high pressure so that its efficiency can be improved and exergetic losses related to heat exchanger are also reduced. This type of configuration offer an efficiency of about 50 to 60 percent by assuming

conventional TIT and SOFC operating temperature about 900 to 1000 C. The direct integration configuration is shown in figure 5.2.

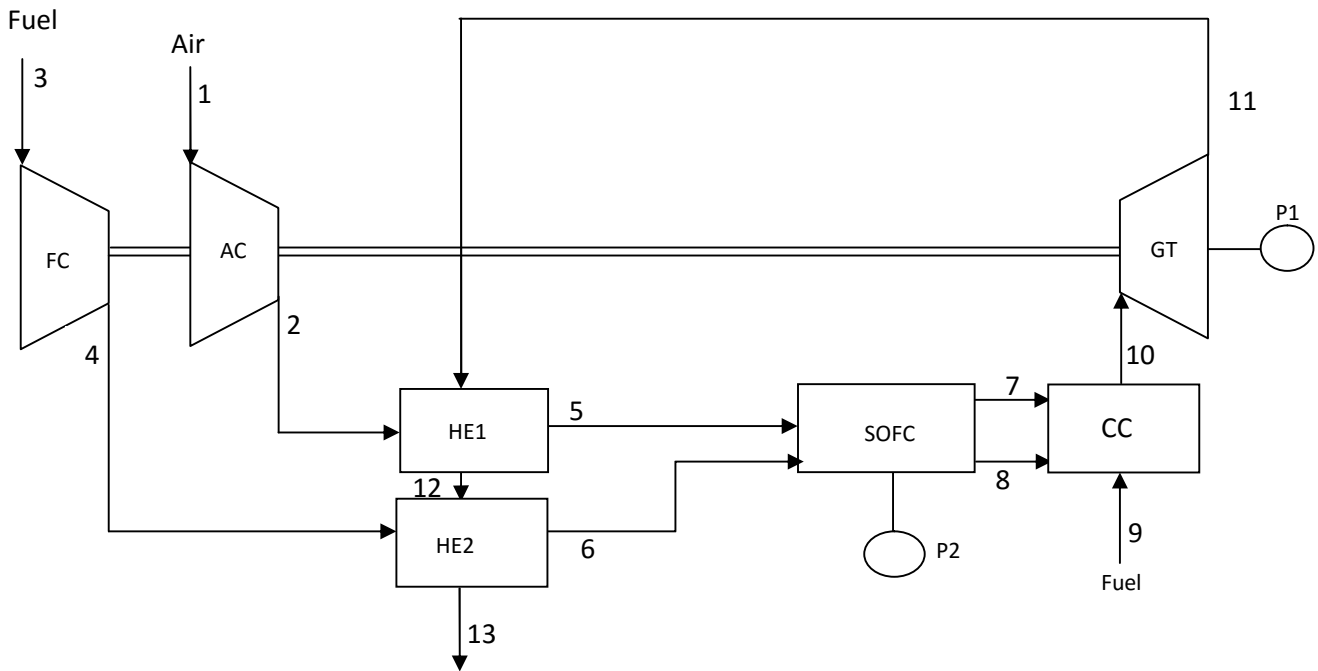


Figure 5.2 Flow Diagram of Direct Integration hybrid systems

**Table 5.2.State points and abbreviation for direct integration hybrid system**

AC	Air Compressor
FC	Fuel Compressor
HE1	Heat exchanger 1
HE2	Heat exchanger 1
SOFC	Solid oxide fuel cell
CC	Combustion Chamber
GT	Gas turbine
P1	Electrical power output from gas turbine
P2	Electrical power output from SOFC

State 1	Inlet to air compressor
State 2	Outlet from air compressor and inlet to Heat exchanger 1
State 3	Inlet to fuel compressor
State 4	Outlet from fuel compressor and inlet to Heat exchanger 2
State 5	Air leaving the heat exchanger 1 and entering into fuel cell
State 6	fuel leaving the heat exchanger 2 and entering into fuel cell
State 7	Depleted air leaving fuel cell and entering into combustion chamber
State 8	Mixture of gases leaving fuel cell and entering into combustion chamber
State 9	Fuel supply into combustion chamber to achieve the desired turbine inlet temperature
State 10	Mixture of gases leaving combustion chamber and entering into gas turbine
State 11	Mixture of gases leaving gas turbine and entering into heat exchanger 1
State 12	Mixture of gases leaving heat exchanger 1 and entering into heat exchanger 2
State 13	Mixture of gases leaving heat exchanger 2 and entering into atmosphere

### 5.3 Application of Hybrid system

The world's first SOFC/GT hybrid system was delivered to Southern California Edison to operate at Irvin's national Fuel Cell research centre. In this system a SOFC pressurized module is integrated with MGT. The system delivered total power output of 220 kilowatt with SOFC has 200 kilowatts and remaining is from MGT. Efficiency is approximate 55 percent. The main application areas of Hybrid SOFC/GT system are as follows:

1. Residential application: To warm the buildings
2. Small industrial application: production of electricity to few Watts
3. Public Buildings: can be used in refrigeration and air conditioning
4. Micro and Macro level power plant

## 5.4 System selection for Analysis

In the thesis work selected system configuration is shown in figure 5.3. On the basis of mathematical modelling presented in previous chapters 3 (for gas turbine) and 4 (for solid oxide fuel cell), a computer programme is developed. This program is developed in engineering equation solver software and simulation is performed. Figure 5.3 is the information flow diagram of the hybrid system used for present analysis.

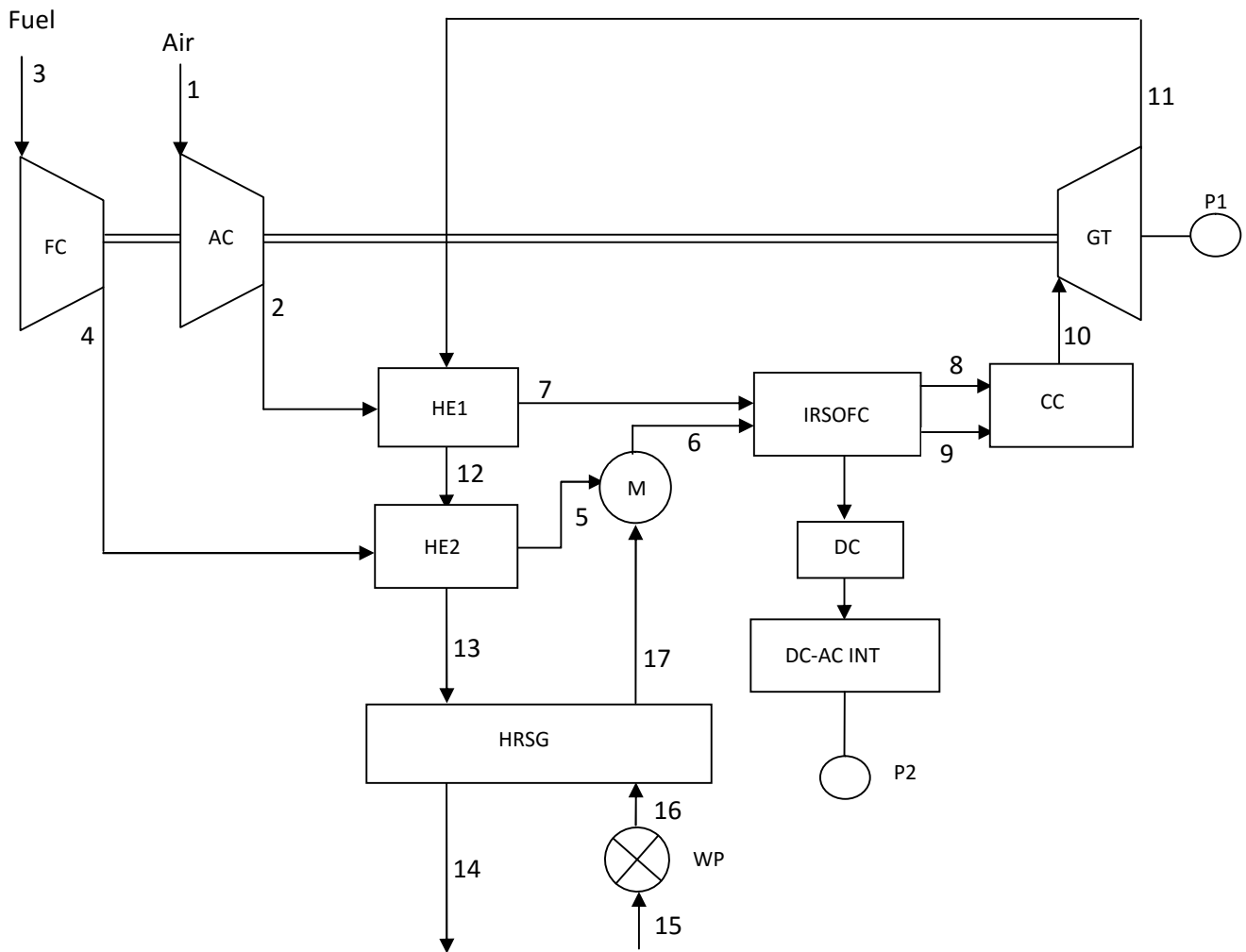


Figure 5.3 Flow diagram for Hybrid System selected for analysis

**Table 5.3.State points and abbreviation for selected hybrid system configuration for analysis**

AC	Air compressor
FC	Fuel compressor
HE1	Heat exchanger 1
HE2	Heat exchanger 1
HRSG	Heat recovery steam generator
WP	Water pump
M	Mixer
IRSOFC	Internal reforming solid oxide fuel cell
CC	Combustion chamber
GT	Gas turbine
DC	Direct current
AC	Alternating current
DC-AC INT	DC To AC Converter Or Inverter
P1	AC power output from gas turbine
P2	AC power output from Solid oxide fuel cell
State 1	Inlet to air compressor
State 2	Outlet from air compressor and inlet to Heat exchanger 1
State 3	Inlet to fuel compressor
State 4	Outlet from fuel compressor and inlet to Heat exchanger 2
State 5	Fuel leaving the heat exchanger 2 and entering into mixer
State 6	Mixer outlet
State 7	Compressed air leaving Heat exchanger 1 and entering into Internal reforming solid oxide fuel cell
State 8	Air at outlet of Fuel cell cathode electrode
State 9	Mixture of gases at outlet of fuel cell anode electrode
State 10	Mixture of gases leaving combustion chamber and entering into gas turbine
State 11	Mixture of hot gases leaving gas turbine after expansion and entering into heat exchanger 1



State 12	Mixture of hot gases leaving heat exchanger 1 and entering into heat exchanger 2
State 13	Mixture of hot gases leaving heat exchanger 2 and entering into heat recovery steam generator
State 14	Mixture of hot gases leaving heat recovery steam generator and entering into atmosphere
State 15	Water enters into water pump
State 16	Compressed water leaving water pump and entering into heat recovery steam generator
State 17	Steam leaving heat recovery steam generator and entering into mixer

**Table 5.4 Flow information for hybrid system selected for analysis**

Compressor parameter	Inlet condition such as pressure ratio, compressor isentropic efficiency and mechanical efficiency is specified
Water pump parameter	Inlet condition such as pressure ratio, pump isentropic efficiency and mechanical efficiency is specified
Heat exchangers and heat recovery steam generator parameter	All heat exchangers and HRSG have tube in tube counter flow arrangement. Effectiveness as an input is specified and outlet conditions of stream are determined on the basis of effectiveness. For calculating properties of outlet stream, equation of effectiveness and energy balance equation are solved simultaneously.
Mixer parameter	The temperature of fuel-steam mixture at mixer outlet is calculated by assuming change in entropy is zero
SOFC parameter	Calculation of polarization losses and cell power is done by taking all Geometric dimension as an input for the analysis of SOFC
Combustion chamber parameter	SOFC outlet condition acts as the input for combustion chamber. Other input such as combustion efficiency, fuel lower calorific value is specified. The temperature and composition of outlet stream is calculated by assuming complete combustion.
Gas turbine parameter	Outlet pressure of gas turbine is specified and power output is determined
Chemical exergy	The chemical exergy for various substance is calculated by providing

	chemical exergy value at reference condition (Table 5.5)
Programme execution	Programme is executed. All desired parameters such as cell theoretical voltage, Voltage losses, Actual cell voltage, Cell power output, Turbine power output, first law efficiency, second law efficiency, exergy at various state points, exergy destruction in various components and properties of working fluid such as pressure, temperature, entropy, enthalpy, molar fraction, molar flow rate etc are calculated by the execution of programme.

**Table 5.5 Standard molar chemical exergy (kJ/kmol) of various substances at  $T_0$  (298.15 K) and  $P_0$  (1.01325 bar) [41]**

Substance	Formula	Model I	Model II
Nitrogen	$N_2(g)$	639	720
Oxygen	$O_2(g)$	3,951	3,970
Carbon dioxide	$CO_2(g)$	14,176	19,870
Water	$H_2O(g)$	8,636	9,500
Water	$H_2O(l)$	45	900
Carbon (graphite)	$C(s)$	404,589	410,260
Hydrogen	$H_2(g)$	235,249	236,100
Sulfur	$S(s)$	598,158	609,600
Carbon monoxide	$CO(g)$	269,412	275,100
Nitrogen monoxide	$NO(g)$	88,851	88,900
Sulfur dioxide	$SO_2(g)$	301,939	313,400
Nitrogen dioxide	$NO_2(g)$	55,565	55,600
Hydrogen peroxide	$H_2O_2(g)$	133,587	-----
Hydrogen sulfide	$H_2S$	799,890	812,000
Ammonia	$NH_3(g)$	336,684	337,900
Oxygen	$O(g)$	231,968	233,700
Hydrogen	$H(g)$	320,822	331,300
Nitrogen	$N(g)$	453,821	-----
Methane	$CH_4(g)$	824,348	831,650
Acetylene	$C_2H_2(g)$	-----	1,265,800
Ethylene	$C_2H_4(g)$	-----	1,361,100
Ethane	$C_2H_6(g)$	1,482,033	1,495,840
Propylene	$C_3H_6(g)$	-----	2,003,900
Propane	$C_3H_8(g)$	-----	2,154,000
n-Butane	$C_4H_{10}(g)$	-----	2,805,800
n-Pentane	$C_5H_{12}(g)$	-----	3,463,300
Benzene	$C_6H_6(g)$	-----	3,303,600
Octane	$C_8H_{18}(l)$	-----	5,413,100
Methanol	$CH_3OH(g)$	715,069	722,300
Methanol	$CH_3OH(l)$	710,747	718,000
Ethyl alcohol	$C_2H_5OH(g)$	1,348,328	1,363,900
Ethyl alcohol	$C_2H_5OH(l)$	1,342,086	1,375,700

**Table 5.6 Input Parameters**

S. No.	Parameters	Value
1	Gas-air heat exchanger effectiveness	0.80
2	Gas-fuel heat exchanger effectiveness	0.80
3	Gas-superheated steam heat exchanger effectiveness	0.80
4	Combustor efficiency	0.98
5	Electric generator efficiency	0.98
6	Inverter efficiency	0.95
7	Air compressor isentropic efficiency	0.80
8	Air compressor mechanical efficiency	0.98
9	Fuel compressor isentropic efficiency	0.80
10	Fuel compressor mechanical efficiency	0.98
11	Pump isentropic efficiency	0.80
12	Pump mechanical efficiency	0.98
13	Gas turbine isentropic efficiency	0.80
14	Gas turbine mechanical efficiency	0.98
15	Limiting Current density(A/m <sup>2</sup> )	9000
16	Methane inlet molar flow rate (kmol/s)	0.0028
17	Water inlet molar flow rate (kmol/s)	0.0057
18	Oxygen inlet molar flow rate (kmol/s)	0.0070
19	Cell operating pressure(bar)	7x1.013
20	Environment pressure (bar)	1.013
21	Environment temperature(°C)	25
22	Fuel utilization factor (%)	85
23	Minimum steam to carbon ratio	2
24	Cell current density (A/m <sup>2</sup> )	1000
25	Anode thickness(cm)	0.010
26	Cathode thickness(cm)	0.220
27	Interconnection thickness(cm)	0.004
28	Anode activation energy (kJ/kmol)	110000
29	Cathode activation energy (kJ/kmol)	160000
30	Pre exponential factor for Anode(A/m <sup>2</sup> )	2.13x10 <sup>8</sup>
31	Pre exponential factor for Cathode (A/m <sup>2</sup> )	1.49x10 <sup>8</sup>

# CHAPTER 6

## Result and Discussion

Based upon the mathematical modelling and simulation of fuel cell and gas turbine hybrid system through programming, calculation has performed. In this chapter result discussion has done.

### 6.1 Program validation

The program which is developed in thesis work has been validated for fuel cell operating voltage and electrical efficiency of hybrid system based upon the supplied input parameters. To get the input parameters many literatures are studied because each data is not available in single literature. The input parameters have been selected from various literatures. The main results obtained from simulation run are presented in Table 6.1. Value of various parameters for each state point which is obtained from execution of programme is summarized in Table 6.2.

*Table 6.1 Results*

<b>Components</b>	<b>Present model</b>	<b>Literatures</b>
Cell Operating Voltage	0.626 V	0.62 V [40]
Cell Power output	1.093 MW	.....
Turbine power output	0.3957 MW	.....
Total power output	1.488 MW	1.5 MW [37]
First law electrical efficiency of hybrid system	66.25	62.2% [39]
Second law efficiency of hybrid system	63.23	.....
Total system exergy	0.485 MW	.....

**Table 6.2 Various output parameters obtained for each state point thermodynamic properties from execution of programme**

<b>S.No.</b>	<b>Chemical exergy (kJ/kmol)</b>	<b>Physical exergy (kJ/kmol)</b>	<b>Enthalpy (kJ/kmol)</b>	<b>Temperature (°C)</b>	<b>Molar flow rate (kmol/s)</b>	<b>Pressure (bar)</b>
1	1301	0	0	25	0.0350	1.013
2	1301	7161	8046	296.3	0.0350	7.093
3	824348	0	-74595	25	0.0028	1.013
4	824348	6543	-67091	209.4	0.0028	7.093
5	824348	15512	-50140	519.6	0.0028	7.093
6	280540	17989	23998	485	0.0084	7.093
7	1301	18667	26085	857.9	0.0350	7.093
8	919.2	24111	33216	1073	0.0305	7.093
9	49856	29021	-187515	1073	0.0140	7.093
10	3350	36988	-23074	1430	0.0434	7.093
11	3350	19206	-39828	998.3	0.0434	1.2
12	3350	8746	-54376	597.1	0.0434	1.2
13	3350	8033	-55469	565.5	0.0434	1.2
14	3350	3560	-63105	338.1	0.0434	1.2
15	45	0	1889	25	0.0056	1.013
16	45	14.58	1903	25	0.0056	7.093
17	8636	19251	61077	457.4	0.0056	7.093

## 6.2 Exergy destruction in various components

Exergy for various components are calculated. Then exergy destruction is calculated. The values of exergy destruction for various components are listed in Table 6.3. From Table 6.3 it is clearly observed that maximum exergy destruction occurs in the solid oxide fuel cell and in the combustion chamber. The reason behind this is very clear. In SOFC it is because of chemical reaction and in combustion chamber it is because of combustion reaction. Due to the chemical and combustion reactions there is a change in compositions of the substance which leads into maximum exergy destruction. Minimum exergy destruction occurs in water pump.

**Table 6.3 Exergy Destruction in various components**

<b>Components</b>	<b>Exergy destruction (kW)</b>	<b>Exergy Destruction %</b>
Water Pump	0.08165	0.016
Mixture	0.1307	0.026
Fuel Compressor	3.119	0.642
Heat Exchanger 2	5.789	1.192
Air compressor	36.71	7.561
Heat recovery steam generator	38.3	7.887
Gas turbine	44.61	9.185
Heat Exchanger 1	51.25	10.55
Combustion chamber	119.2	24.55
Solid oxide fuel cell	186.4	38.39
<b>Total Exergy Destruction</b>	<b>485.5 kW</b>	

## 6.3 Thermal analysis based upon the simulation

### 6.3.1 Effect of current Density:

The entire performance of fuel cell is governed by the current and voltage relationship, so it is very important to study the behavior of cell with respect to cell current density. Effect of variation in current density on cell voltage is shown in figure 6.1. The maximum cell voltage occurs at zero current density (also known as open circuit voltage). With the increase in current density, cell voltage decreases. It observed that at low temperature voltage decreases rapidly with increases in current density as compared to high operating temperature.

From figure 6.2 it is clear that activation loss is predominant at low current density, it increases at low current density between 0-3000 A/m<sup>2</sup> and at higher current density the increase is less as compared to low current density.

From figure 6.3 it is observed that ohmic loss is linearly dependent on current density. Ohmic loss is governed by Ohm's law. For a particular cell Ohmic loss decreases or increases only when current density changes or operating temperature of fuel cell changes as the resistivity depends upon the operating temperature only.

Effect of variation in current density on Concentration loss is shown in figure 6.4. At low current density, concentration loss is less dominant as compared to higher current density. It dramatically increases at higher current density. Concentration loss reduces with the decrease in the temperature but not very significant effect observed.

From figure 6.5 it is observed that initially Power density increases with increase in the current density reaches to peak value and then started decreasing with increase in current density. The maximum power density of about 1500 W/m occurs in nearly mid values of 6000-8000 A/m<sup>2</sup> of current density.

The efficiency of hybrid system decreases with increasing current density (Figure 6.6). Major fraction of power output (almost 70 %) of the hybrid system is contributed by fuel cell. The power output of fuel cell depends upon the voltage and current.

From figure 6.7, it is clear that cell power decreases with increase in current density. Minimum cell power occurs at 5000 A/m<sup>2</sup> current density.

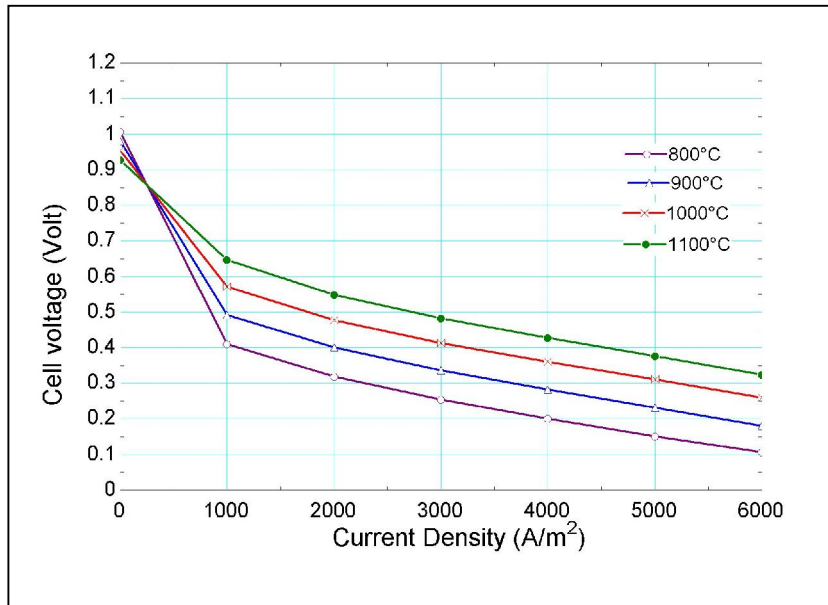


Figure 6.1 variation of cell operating voltage with current density

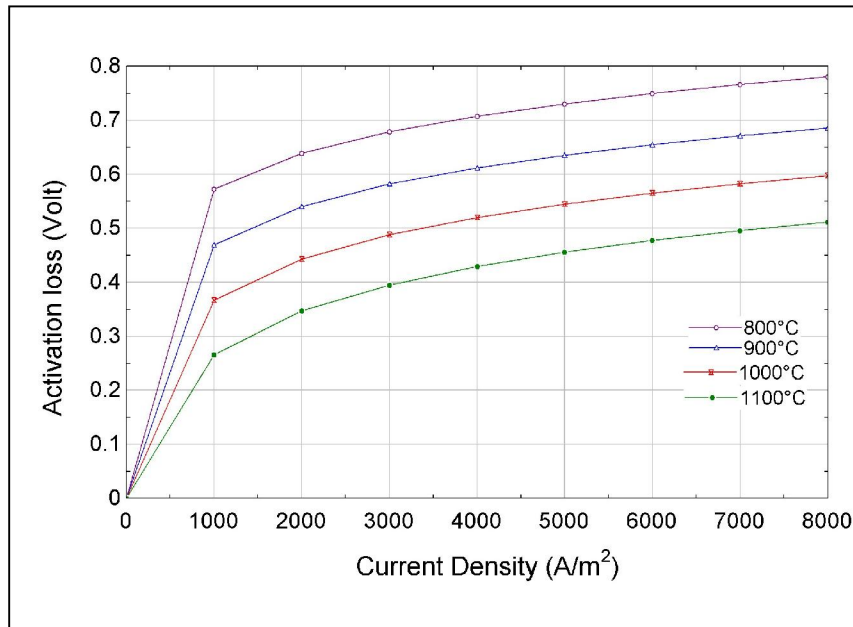


Figure 6.2 variation of Activation loss with current density



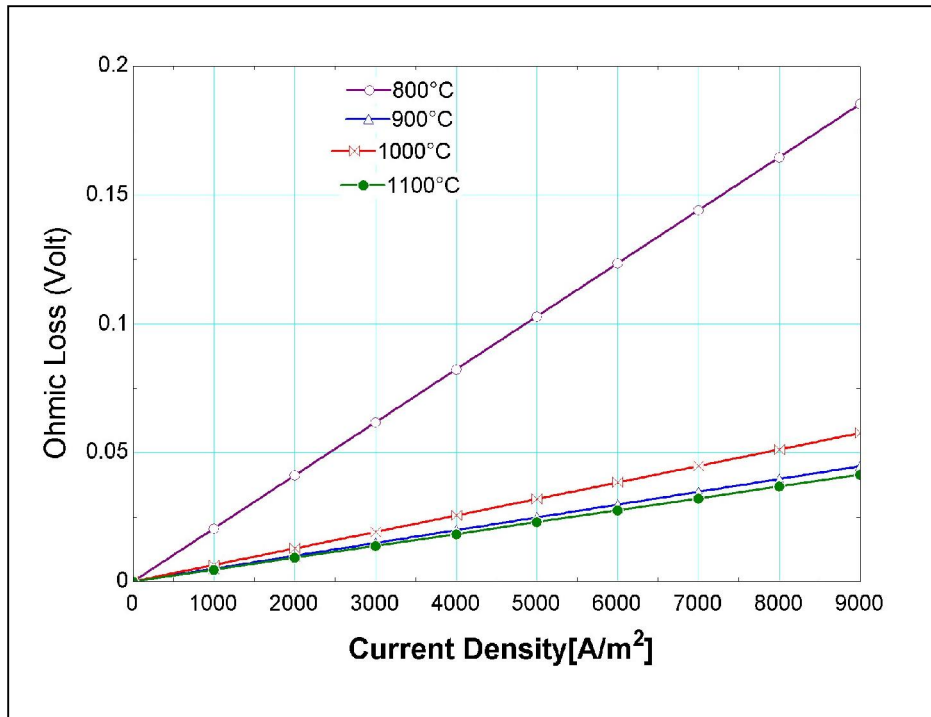


Figure 6.3 Variation of Ohmic loss with current density

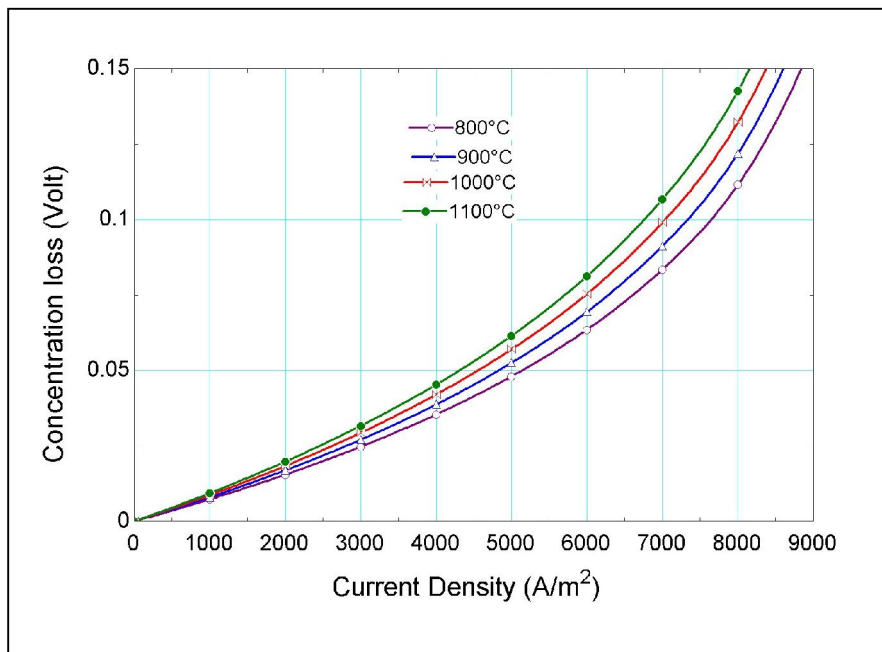


Figure 6.4 Variation of Concentration loss with current density

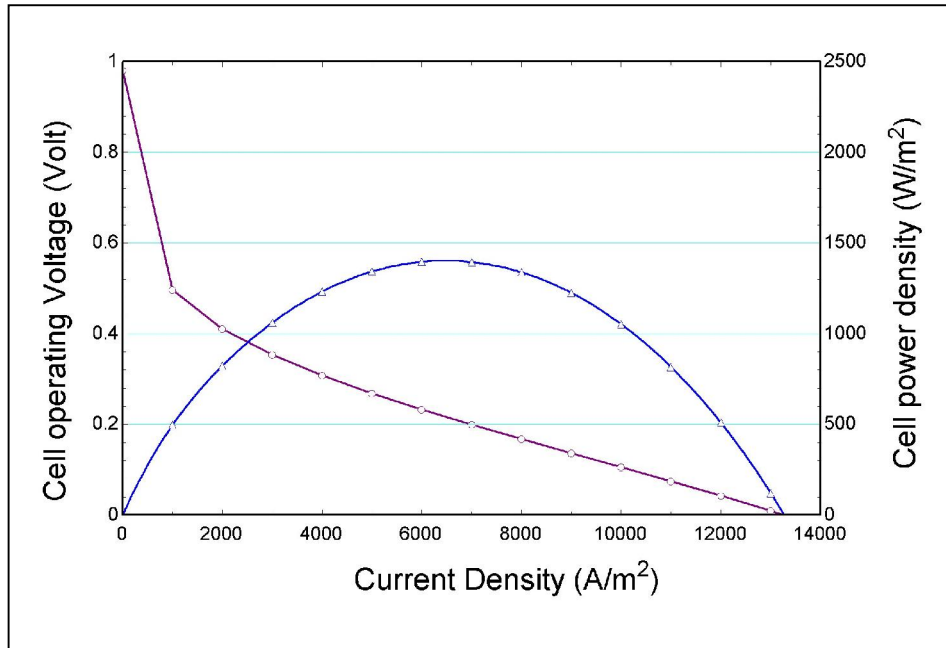


Figure 6.5 Variation of Power density and voltage with current density

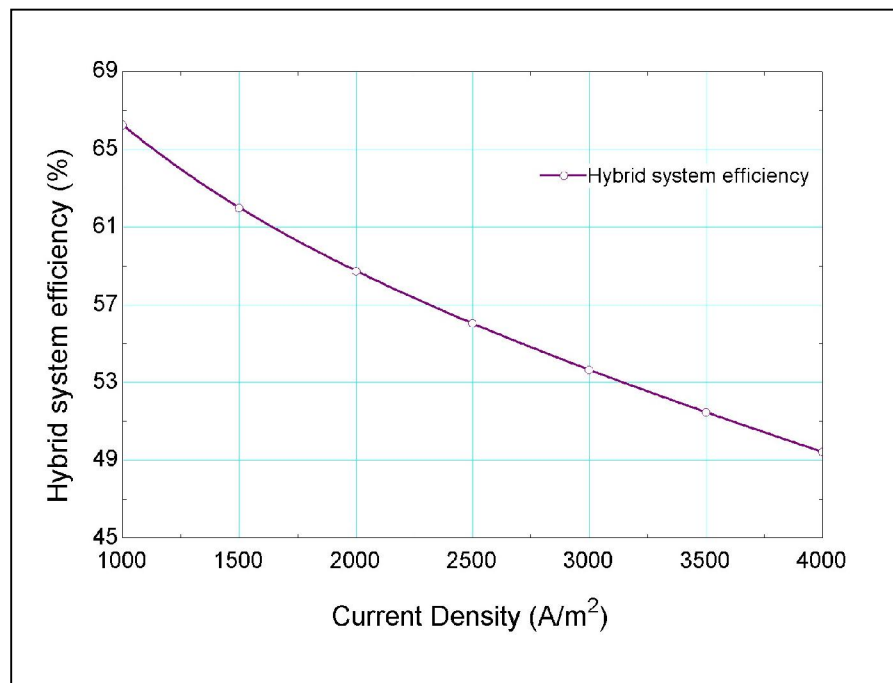


Figure 6.6 Variation of Efficiency with current density

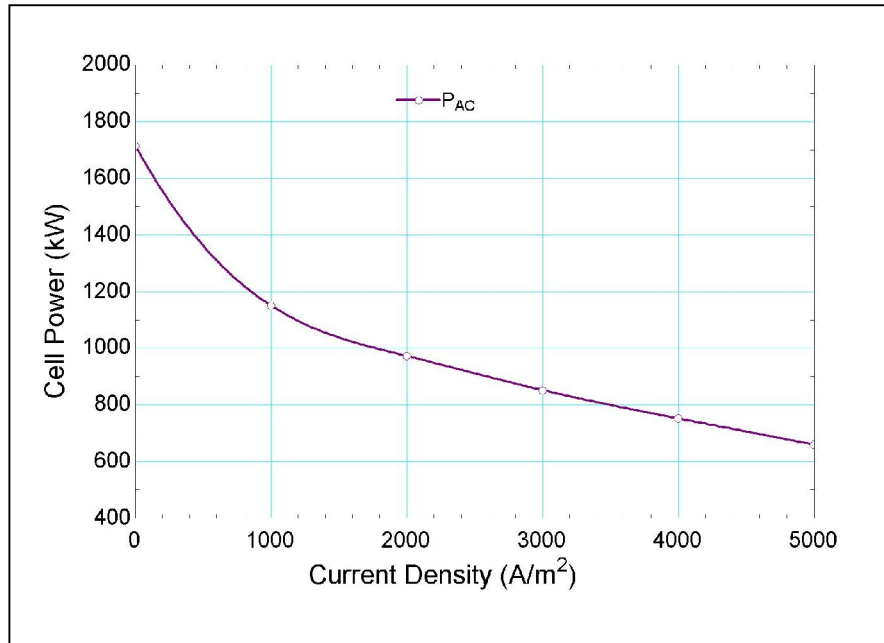


Figure 6.7 Variation of Cell AC power with current density

### 6.3.2 Effect of Fuel flow rate:

From figure 6.8, it is clear that turbine work output increases with increasing fuel flow. With the variation of fuel flow between 0.0028 - 0.005 kmol/s, Turbine power output varies from about 390 to 670 kW. Similarly fuel cell power output increases with increasing fuel flow. With increasing fuel flow rate from 0.0028 - 0.005 kmol/sec, cell AC power output varies from about 1050 to 1850 kW. Higher fuel flow rate means more conversion from chemical energy to electrical energy so more current will be produced and thus raise the cell power output. With increase in the fuel flow rate, the cell operating temperature is also increases which increases the cell exhaust temperature and thus increases turbine power output.

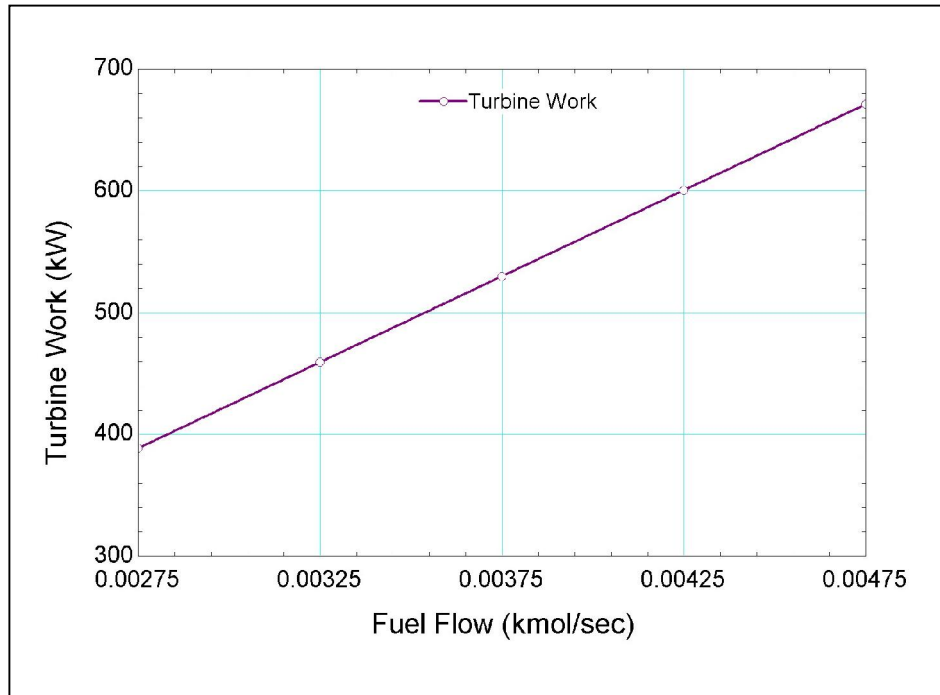


Figure 6.8 Variation of Turbine work with Fuel flow rate

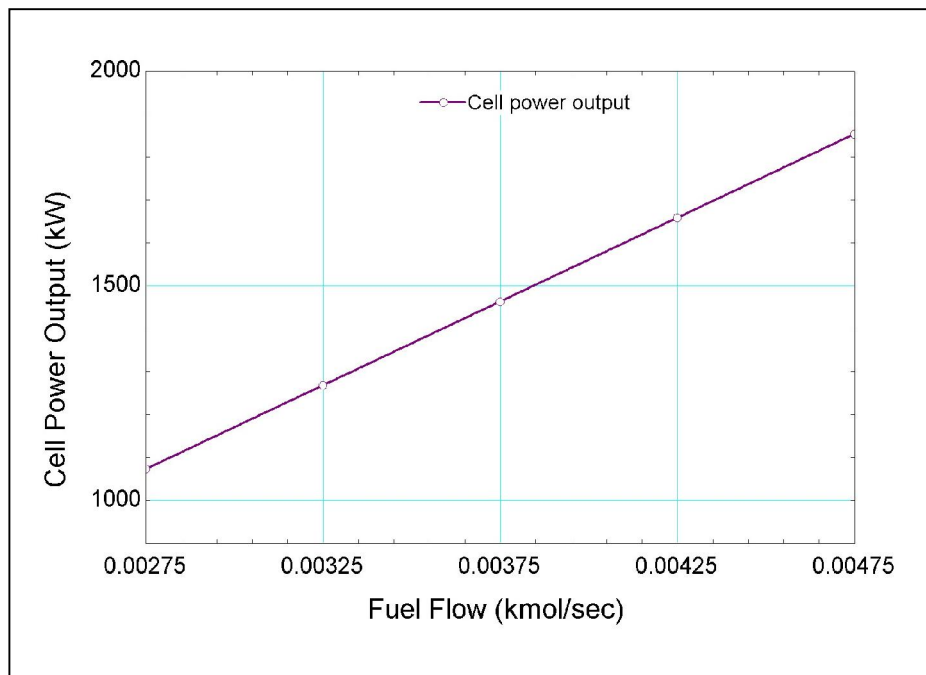


Figure 6.9 Variation of Cell AC power with Fuel flow rate

### 6.3.3 Effect of fuel utilization efficiency:

Figure 6.10 clearly explains that higher the fuel utilization efficiency higher the electrical efficiency. When the fuel utilization factor is very high it has an advantage that almost all hydrogen which is produced by the internal reforming reactions is consumed within the fuel cell during the electrochemical reaction. Thus, fuel cell produces more electricity.

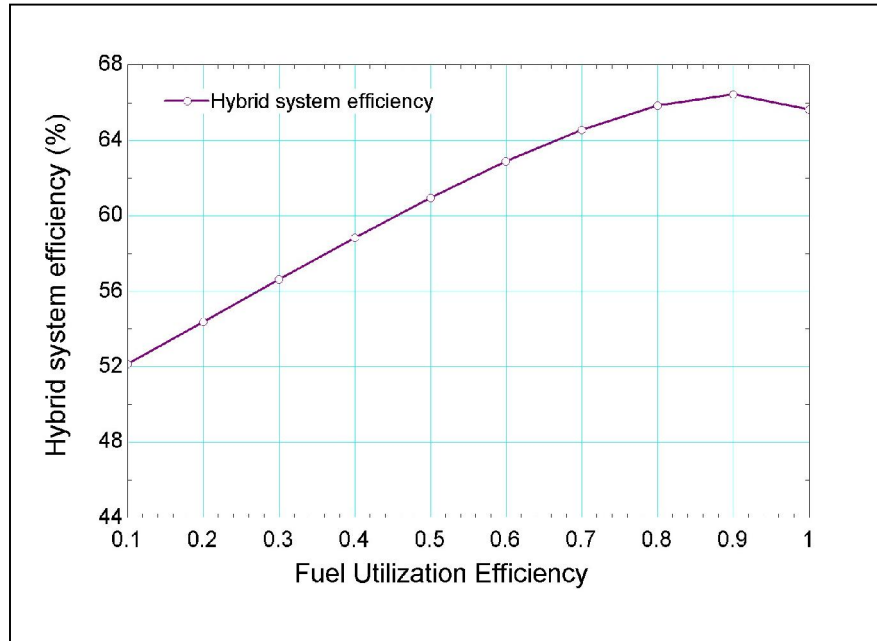


Figure 6.10 Variation of Hybrid system efficiency with Fuel utilization efficiency

### 6.3.4 Effect of cell operating temperature:

Figure 6.11 and figure 6.12 show the effect of cell operating temperature on the hybrid system efficiency and power output respectively. Hybrid system efficiency increases from about 43 to 69% with increasing the temperature from 800 to 1100°C.

Both the cell power output and gas turbine power output increases with increasing cell operating temperature. Effect of Cell operating temperature on cell power output is more as compared to gas turbine power output.

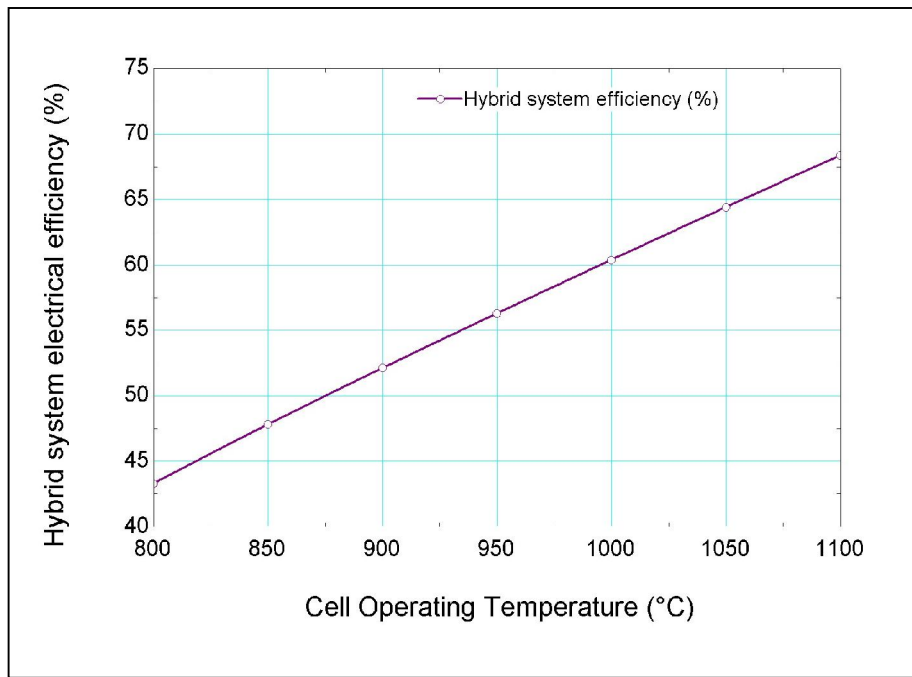


Figure 6.11 Variation of Hybrid system efficiency with Cell operating temperature

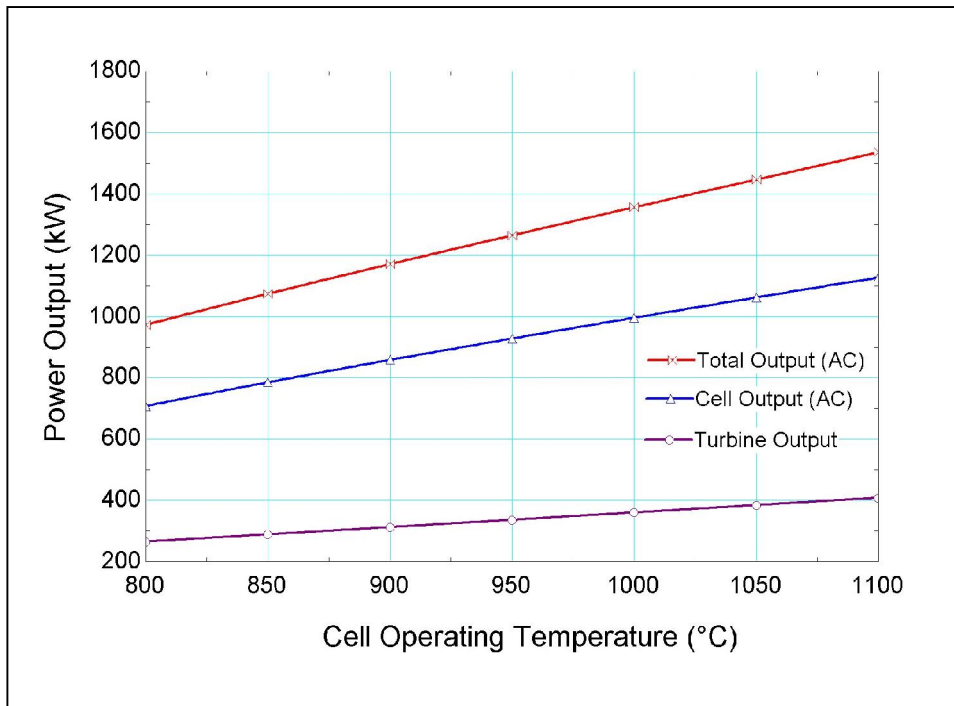


Figure 6.12 Variation of Power output with Cell operating temperature

### **6.3.5 Effect of pressure ratio:**

Figure 6.13 to figure 6.18 shows the variation of Hybrid system efficiency, Turbine power output, cell power output and cell voltage with the pressure ratio. Pressure ratio here is the ratio of pressure at outlet of compressor to the pressure at the inlet of compressor. For simplicity pressure for both the fuel compressor and air compressor is taken as same.

From figure 6.13, it is clear that hybrid system efficiency increases with increasing the pressure ratio. Although increasing the pressure ratio also increase the power requirement for compressors but it also improve the output from fuel cell and turbine. So overall output increases subsequently efficiency increases.

Figure 6.14 clearly show that the cell AC output increases with increasing pressure ratio. Increasing the pressure ratio of the compressors increases the flow temperature and consequently increases the cell operating temperature through thermal effect. Higher cell operating temperature means more efficient operation of fuel cell and waste heat will be less generated. The increase in cell temperature increases the cell voltage and so the AC power output from cell also increases. Figure 6.15 shows the increment in the cell voltage with pressure ratio.

Figure 6.16 show that turbine power output increases with increasing pressure ratio. Increase in pressure ratio increases the cell operating temperature and so increase the cell exit flow temperature. Proportionally gas turbine produces more mechanical work through expansion process and with higher flow energy.

Figure 6.17 show that exergy efficiency increases with increasing pressure ratio.

Figure 6.18 shows that exergy destruction for SOFC is decreases with the increase in the pressure ratio while in case of combustion chamber exergy destruction increases slightly with increasing pressure ratio. Increase in exergy destruction in SOFC is more prominent than decreases in combustion chamber.

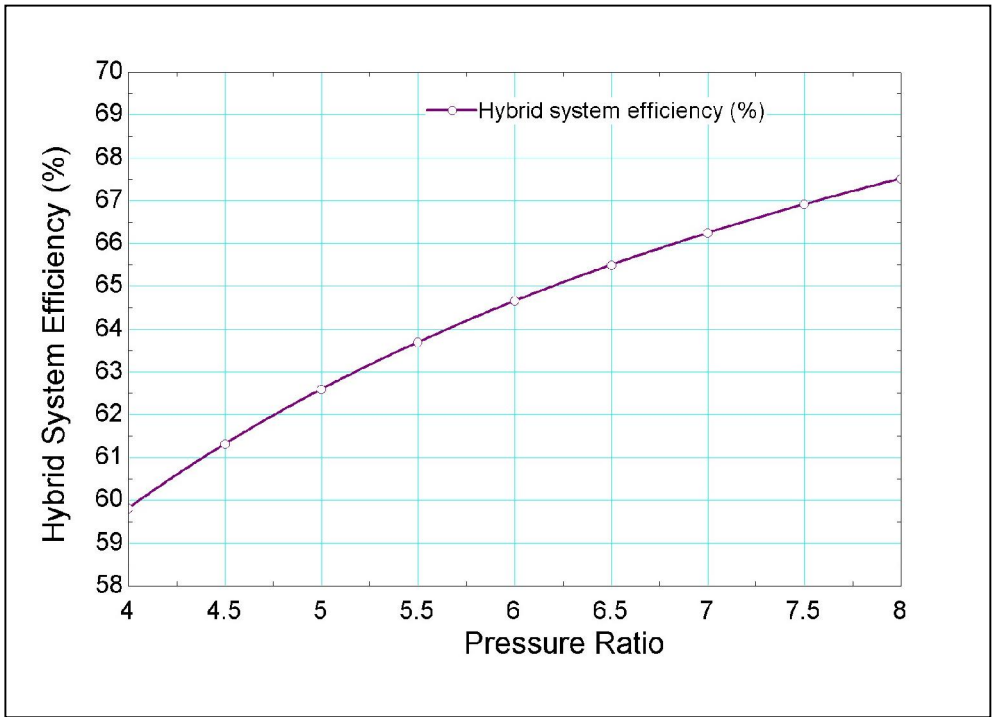


Figure 6.13 Variation of Hybrid system efficiency with Pressure ratios of compressor

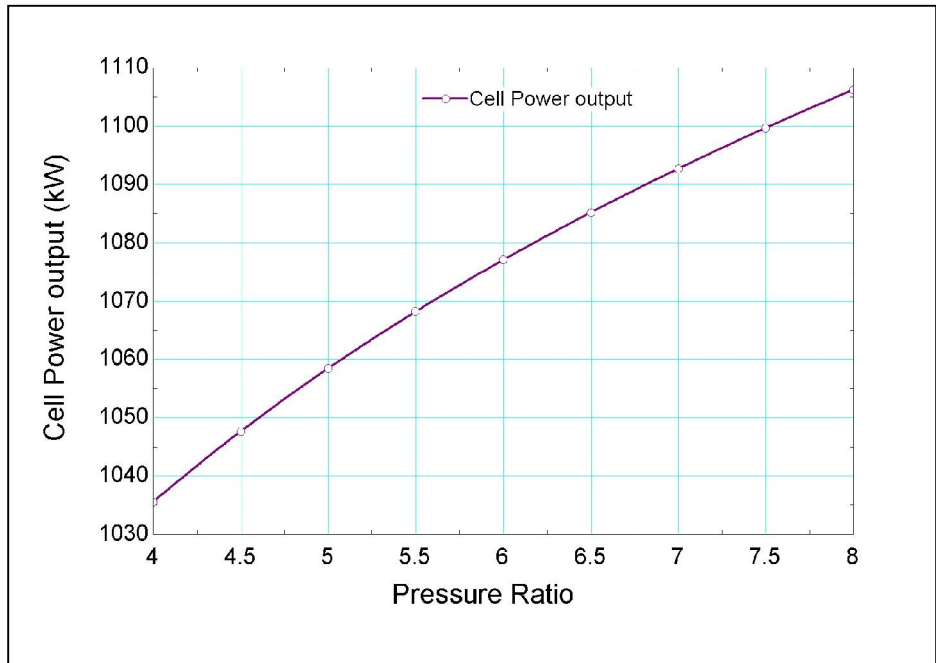


Figure 6.14 Variation of cell power output with Pressure ratios of compressor



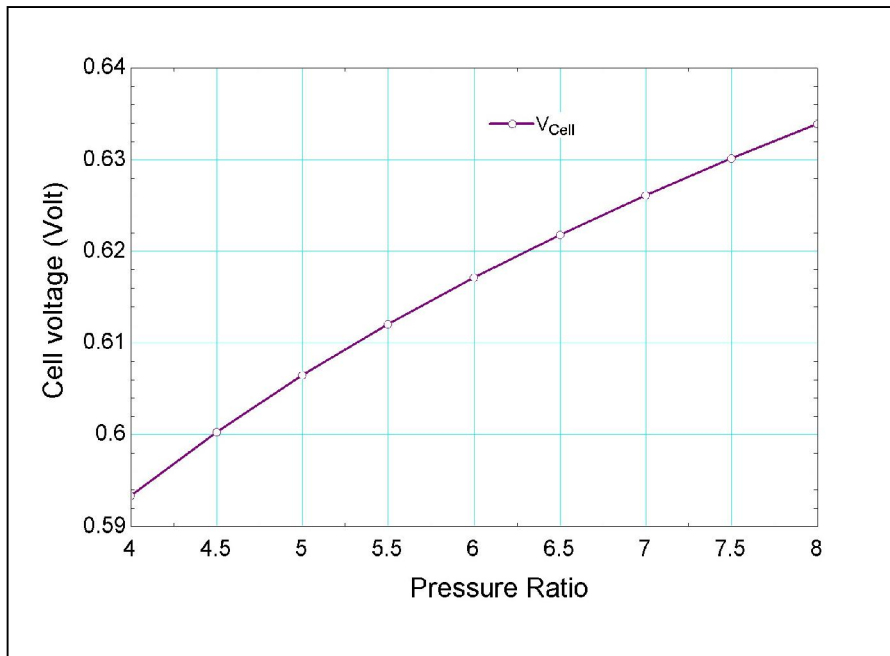


Figure 6.15 Variation of cell voltage with Pressure ratios of compressor

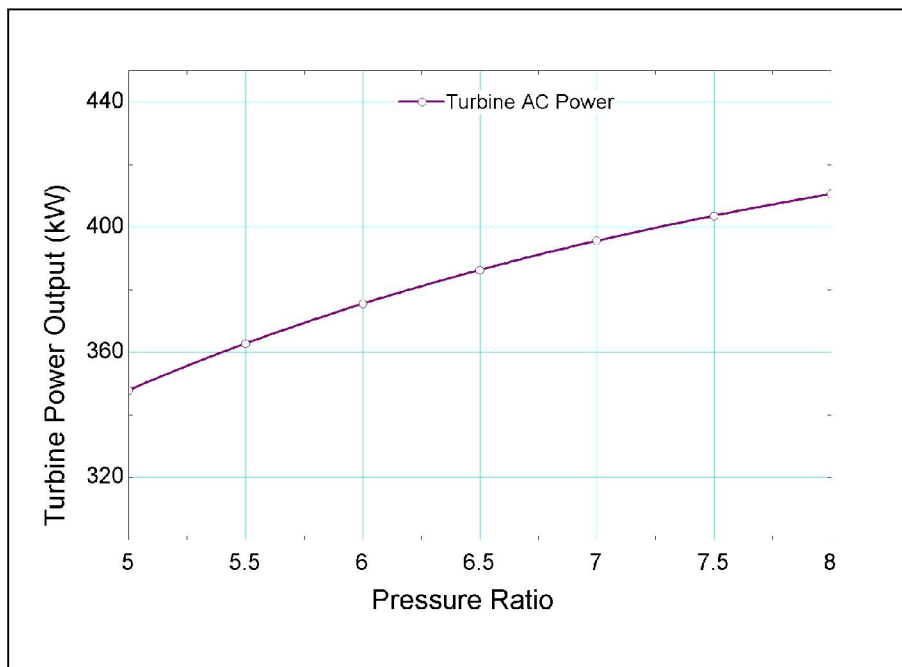


Figure 6.16 Variation of Turbine power output with Pressure ratios of compressor

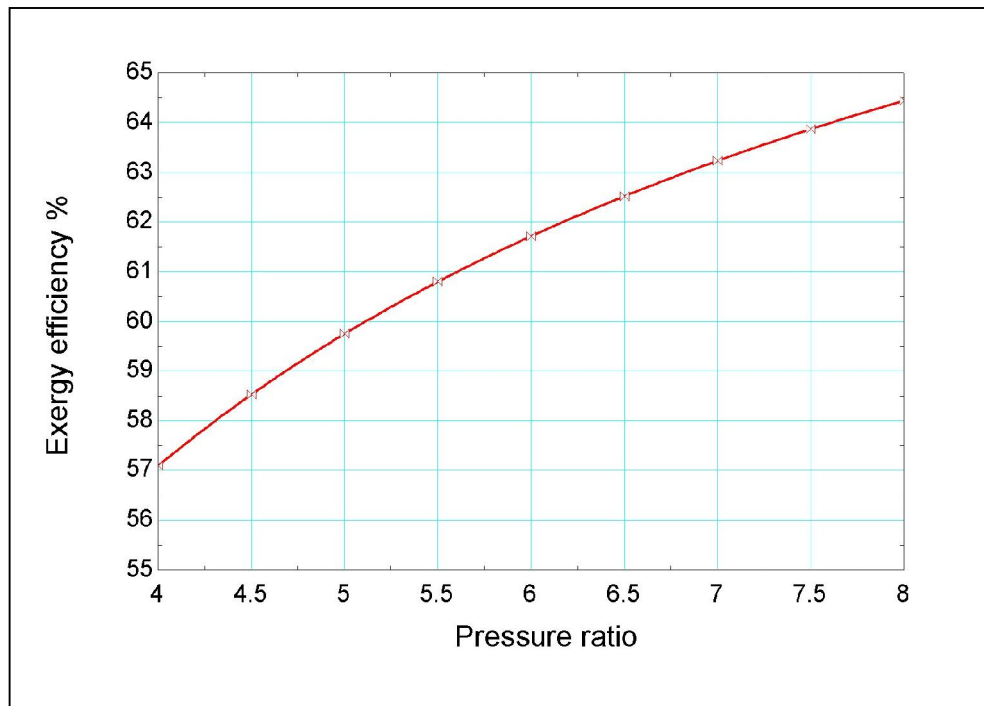


Figure 6.17 Variation of exergy efficiency with Pressure ratios of compressor

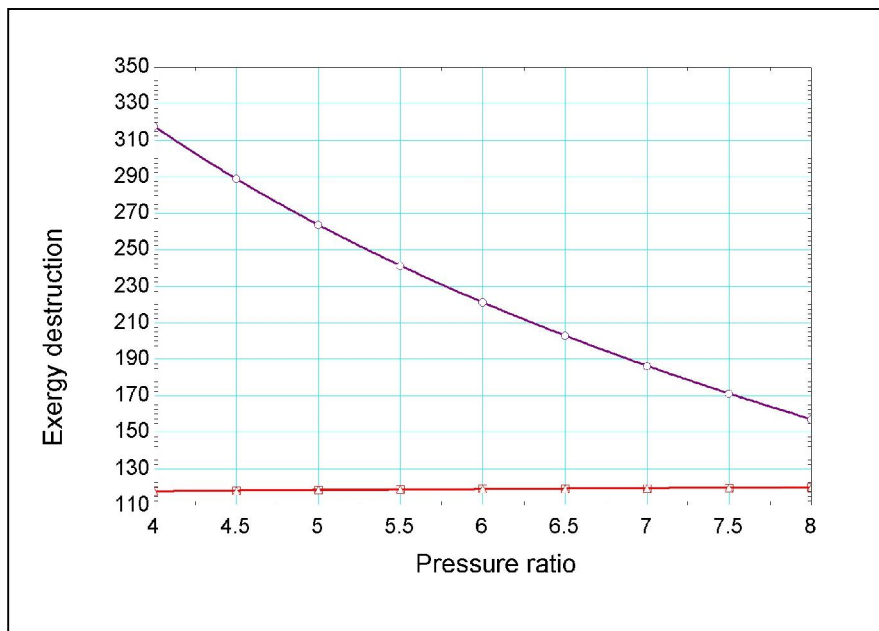


Figure 6.18 Variation of exergy destruction in SOFC and CC with Pressure ratios of compressor

### 6.3.6 Effect of Turbine Inlet temperature (TIT):

Figure 6.19 and Figure 6.20 shows that energy efficiency and exergy efficiency both are decreasing with increase in Turbine inlet temperature (TIT).

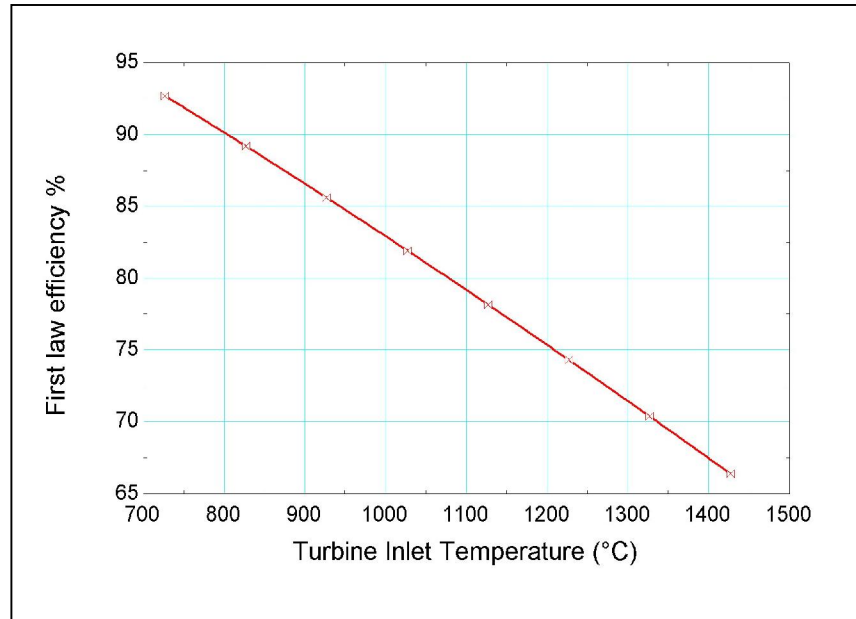


Figure 6.19 Variation of First law efficiency with turbine inlet temperature

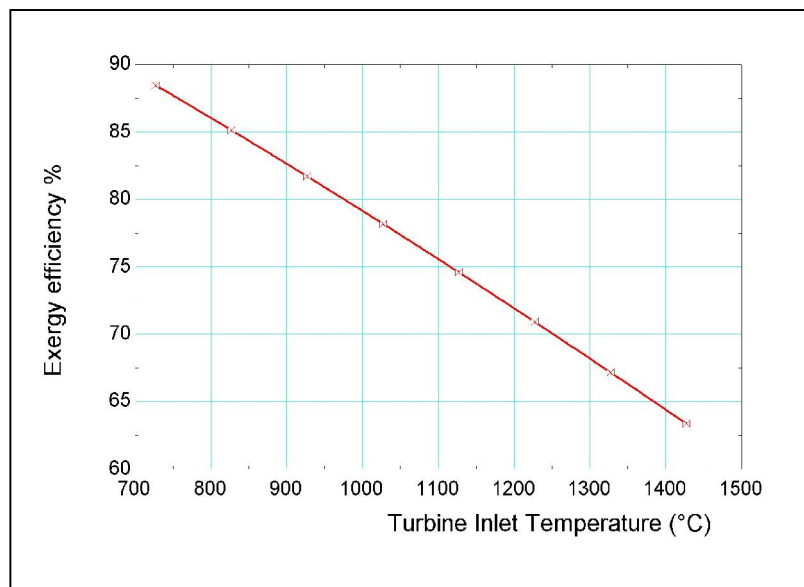


Figure 6.20 variation of exergy efficiency with turbine inlet temperature

# CHAPTER 7

## Conclusion

### **Conclusions:**

Mathematical modelling and simulation of SOFC/GT hybrid system has been done. Effect of parameters on performance of a hybrid SOFC/GT power system was observed. The parameters include temperature, pressure, the cathode flow rate, the anode flow rate, and percentage of fuel use. Power production and the first and second law efficiencies of the hybrid SOFC/GT are calculated. Hybrid system first law electrical efficiency is 66.25; Hybrid system second law efficiency 63.23 and the total electrical power output calculated is 1.488 MW. Exergy of various components in hybrid system is calculated. The maximum exergy destruction occurred in SOFC due to electrochemical reaction. The total exergy destruction computed is 0.485 MW.

# CHAPTER 8

## Recommendation and Scope of future work

This hybrid system has a wide range of application. Simulation makes this system more reliable for commercial purpose. In coming future there is a various scope of work in the field of SOFC/GT hybrid system. These can be as follows:

1. In the present model analysis is done by taking tubular fuel cell geometry. This analysis can be done for more geometry.
2. In the present model we have taken methane as a fuel. In future this system can be modified to use some other gases or mixture of gases such as natural gas or syn- gas
3. We have taken constant value of current density. In future work it can be calculated and this calculated value can be taken for analysis.
4. In the present work we have the waste energy after heat recovery steam generator which is exhausted into atmosphere. In future work a waste heat recovery system at the system exhaust can be considered.
5. In future work, Thermo-economic analysis of the present model can be done.

## **REFERENCE**

- [1] Adam Hahn, "Modelling and control of solid oxide fuel cell-gas turbine power plant systems", Master Thesis, University of Pittsburgh, 2000.
  
- [2] K. F. Kesser, M. A. Hoffman and J. W. Baughn, "Analysis of a Basic Chemically Recuperated Gas Turbine Power Plant, J. Eng. Gas Turbines Power 116 (2), 277-284 (Apr 01, 1994).
  
- [3] Yousef S.H. Najjar, "Gas turbine cogeneration systems: a review of some novel cycles", Applied Thermal Engineering 20(2):179-197, 02/ 2000.
  
- [4] Yousef S.H. Najjar, "Enhancement of performance of gas turbine engines by inlet air cooling and cogeneration system", Applied Thermal Engineering 16(2), 163-173, 1996.
  
- [5] Maria Jonssona, Jinyue yan, "Humidified gas turbines- a review of proposed and implemented cycles", Energy 30; 1013-1078, 2005.
  
- [6] P.A.Pilavachi, "Power generation with gas turbine systems and combined heat and power", Applied Thermal Engineering 20; 1421-1429, 2000.
  
- [7] Stefano Campanari Ph.D., "Thermodynamic model and parametric analysis of a tubular SOFC module", Journal of Power source 92:26-34, 2001.
  
- [8] A. Bharadwaj, D. H. Archer and E. S. Rubin, " Modelling the performance of a Tabular Solid oxide fuel cell", J. Fuel Cell Sci. Technol 2(1), 38-44, 2004.
  
- [9] Maher A. R. Sadiq Al Baghdadi, "Modelling of proton exchange membrane fuel cell performance based on semi-empirical equations", Renewable Energy 30:1587–1599, 2005.
  
- [10] Ananda Himansu, Joshua E. Freeh, Christopher J. Steffen, Jr., Robert T. Tornabene, and Xiao-Yen J. Wang, "Hybrid Solid Oxide Fuel Cell/Gas Turbine System Design for

High Altitude Long Endurance Aerospace Missions”, NASA/TM—2006-214328, FUELCELL2006–97095, May 2006.

- [11] Sadik Kakaça, Anchasa Pramuanjaroenkijb, Xiang Yang Zhou, “A review of numerical modeling of solid oxide fuel cells”, *International Journal of Hydrogen Energy* 32 (2007) 761 – 786.
- [12] Nico Hotz, Stephan M. Senn, Dimos Poulikakos,” Exergy analysis of a solid oxide fuel cell micro power plant” *Journal of Power Sources* 158, 333–347, 2006.
- [13] Eugene L Keating, *Applied Combustion*”, CRC Press, 2<sup>nd</sup> Edition: 2007(page 111).
- [14] Tsang-Dong Chung, Wen-Tang Hong, Yau-Pin Chyou, Dong-Di Yu, Kin-Fu Lin, Chien-Hsiung Lee, “Efficiency analyses of solid oxide fuel cell power plant systems”, *Applied Thermal Engineering*, vol. 28, no. 8, pp. 933-941, 2008.
- [15] Navadol Laosiripojana, Wisitsree Wiyaratn, Worapon Kiatkittipong, Arnornchai Arpornwichanop, Apinan Soottitantawat, Suttichai Assabumrungrat, “Reviews on Solid oxide fuel cell technology” *Engineering Journal*, 13, No. 1 (2009).
- [16] *Marcos V. Moreira and Gisele E. da Silva*, “A practical model for evaluating the performance of proton exchange membrane fuel cells”, *Renewable Energy* 34, 1734-1741, 2009.
- [17] Wayne Doherty, Anthony Reynolds, David Kennedy, “Modelling and Simulation of a Biomass Gasification-solid Oxide Fuel Cell Combined Heat and Power Plant using Aspen Plus”, In 22<sup>nd</sup> International Conference on Efficiency, Cost, Optimization Simulation and Environmental Impact of Energy Systems, Foz do Iguaçu, Paraná, Brazil, August 31 – September 3, 2009.
- [18] Haji Shaker, “Analytical Modelling of PEM Fuel Cell I-V Curve”, *Renewable Energy* 36: 451-458, 2011.

- [19] Jenica ILeana corcau, Liviu Dinca, "On using PEMFC for electrical power generation on more electric aircraft", International journal of electrical, computer, energetic, electronic and communication Engineering, Vol 6, No. 2, 2012.
- [20] Sivan Kartha, Thomas G. Kreutz, and Robert H. Williams, " Small scale biomass fuel cell/Gas turbine power systems for rural areas", Energy for sustainable Development, Volume IV, No. 1 , June 2000.
- [21] Shinji Kimijima and Nobuhide Kasagi, "Performance Evaluation of Gas Turbine-Fuel Cell Hybrid Micro Generation System", ASME Turbo Expo 2002, June 3–6, Amsterdam, The Netherlands.
- [22] Rama S.R. Gorla, Shantaram S. Pai and Jeffrey J. Rusick, "Probabilistic Analysis of Solid Oxide Fuel Cell Based Hybrid Gas Turbine System", NASA/TM—2003-211995, GT–2003–38046, April 2003.
- [23] Said Al-Hallaj, Fuad Alasfour, Sandeep Parekh, Shabab Amiruddin, J. Robert Selman, Hossein Ghezal-Ayagh, "Conceptual design of a novel hybrid fuel cell/desalination system", Elsevier, Desalination, 164, 19–31, 2004.
- [24] R. A. Roberts and J. Brouwer, "Dynamic Simulation of a Pressurized 220kW Solid Oxide Fuel-Cell–Gas-Turbine Hybrid System: Modeled Performance Compared to Measured Results", J. Fuel Cell Sci. Technol 3(1), 18-25 (Aug 19, 2005).
- [25] Senthil V. Vannivedu Umapathi, Kiran Rao Bhimma and Parchuri M. V. Subbarao, "Performance Analysis of Hybrid Solid Oxide Fuel Cell - Gas Turbine Power Generating System", The 2nd Joint International Conference on "Sustainable Energy and Environment (SEE 2006)" 21-23 November 2006, Bangkok, Thailand, 2006
- [26] A. Sordi, E. P. da Silva, A. J. M. Neto, D. G. Lopes, C. S. Pinto, P. D. Araújo, "Thermodynamic simulation of biomass gas steam reforming for a solid oxide fuel cell (sofc) system", Brazilian Journal of Chemical Engineering, Vol. 26, No. 04, pp. 745 - 755, October - December, 2009.
- [27] A. Salogni, P. Colonnab, "Modeling of solid oxide fuel cells for dynamic simulations of integrated systems", Applied Thermal Engineering, 30, 464–477, 2010.



- [28] Denver F. Cheddie, Renique J Murray, "Thermo-economic modeling of an indirectly coupled solid oxide fuel cell/gas turbine hybrid power plant", JOURNAL OF POWER SOURCES 195(24):8134-8140, 2010.
- [29] Bang-Møller Christian, Rokni Masoud, "Thermodynamic Performance Study of Biomass Gasification, Solid Oxide Fuel Cell and Micro Gas Turbine Hybrid Systems", Energy Conversion and Management, 51:2330-2339, 2010.
- [30] Luigi Leto, Celidonio Dispenza, Angelo Moreno, Antonio Calabr`o, "Simulation Model of a Molten Carbonate Fuel Cells - Microturbine Hybrid System", Applied Thermal Engineering, Elsevier, 31 (6-7), 2011. HAL Id: hal-00723974.
- [31] Xiao-Juan Wu, Qi Huang Xin-Jian Zhu, " Thermal modelling of a solid oxide fuel cell and micro gas turbine hybrid power system based on modified LS-SVM", International journal of hydrogen energy 36:885-892,2011.
- [32] C. Zuo, M. F. Liu, M. L. Liu "Solid Oxide Fuel Cells" Chapter 2, Sol-Gel Processing for Conventional and Alternative Energy, Advances in Sol-Gel Derived Materials and Technologies, DOI: 10.1007/978-1-4614-1957-0\_2, Springer Science and Business Media New York 2012.
- [33] Matthew M. Mench," Fuel Cell Engines", John Wiley & Sons, 2008.
- [34] Department of Energy U.S," Fuel Cell Handbook", U.S Department of Energy, Office of Fossil Energy, National Energy Technology Laboratory, 5<sup>th</sup> Edition 2000.
- [35] Matias Halinen, "Improving the performance of solid oxide fuel cell systems", ISBN 978-951-38-8237-2.
- [36] Sadeqh Motahar, Ali Akbar Alemrajabi, "Exergy based performance analysis of a solid oxide fuel cell and steam injected gas turbine hybrid power system", International journal of Hydrogen Energy 34,2396-2407, 2003.

- [37] F. Calisea,\_, M. Dentice d'Accadiaa, A. Palombo, L. Vanolib "Simulation and exergy analysis of a hybrid Solid Oxide Fuel Cell (SOFC)–Gas Turbine System" *Energy* 31 (2006) 3278–3299.
- [38] S.H. Chan\*, K.A. Khor, Z.T. Xia, "Complete polarization model of a solid oxide fuel cell and its sensitivity to the change of cell component thickness" *Journal of Power Sources* 93 (2001) 130-140.
- [39] S.H. Chan\*, H.K.Ho, Y. Tian, " Modelling of simple hybrid solid oxide fuel cell and gas turbine power plant", *Journal of Power Sources* 109 (2002) 111-120.
- [40] Francesco Calise\*\*, Massimo Dentice d'Accadia and Adolfo Palombo "A Detailed One Dimensional Finite-Volume Simulation Model of a Tubular SOFC and a Pre-Reformer" *Int. J. of Thermodynamics* ISSN 1301-9724, Vol. 10 (No. 3), pp. 87-96, September 2007.
- [41] Adrian Bejan, George Tsatsaronis, Michael Moran, "thermal design and optimization", John Wiley & Sons, inc., 1996.

## APPENDIX 'A'

**Table A.1. Resistivity Constant [36]**

<b>S.NO.</b>	<b>Component</b>	<b>a</b>	<b>b</b>
1	Anode	0.0000298	-1392
2	Cathode	0.0000811	600
3	Electrolyte	0.0000294	10350
4	Interconnector	0.001256	4690

**Table A.2. Fuller diffusion volume**

<b>S.NO.</b>	<b>Gas species</b>	<b>Fuller diffusion volume</b>
1	O <sub>2</sub>	16.6
2	N <sub>2</sub>	17.9
3	H <sub>2</sub>	7.07
4	H <sub>2</sub> O	12.7

## Program for SOFC/GT Hybrid system

```

T||0=298.15[K]
P||0=1.01325[bar]
T||C_0=convertTEMP('K','C',T||0)
R_U=R#
F=96485
Mw_O2=MolarMass(O2)
Mw_CH4=MolarMass(CH4)
Mw_h2=MolarMass(H2)
Mw_CO2=MolarMass(CO2)
Mw_N2=MolarMass(N2)
ex||ch_CH4=824348
ex||ch_H2=235249
ex||ch_water=45
ex||ch_N2=639
ex||ch_O2=3951
ex||ch_CO2=14176
ex||ch_CO=269412
ex||ch_H2O=8636
STCR=2.0
x||N2_1=0.8
x||O2_1=0.2
x||CH4_3=1
n||CH4_3=0.0028[kmol/s]
n||CH4_6=n||CH4_3
n||Tot_1=0.035
n||N2_1=n||Tot_1*x||N2_1
n||H2O_15=STCR*n||CH4_3
n||Tot_6=n||CH4_3+n||H2O_15
x||CH4_6=n||CH4_3/n||Tot_6
x||H2O_6=n||H2O_15/n||Tot_6
x||O2_8=n||O2_8/n||Tot_8
x||N2_8=n||N2_1/n||Tot_8
n||Tot_9=n||Tot_6+2*x
n||Ch4_9=n||CH4_3-x
n||CO_9=n||CO_6+x-y
n||H2_9=n||H2_6+3*x+y-z
n||H2O_9=n||H2O_15-x-y+z
n||CO2_9=n||CO2_6+y
n||H2_6=0
n||Tot_15=n||water_15
n||Tot_4=n||Tot_3
n||Tot_5=n||Tot_4
n||Tot_6=n||Tot_5+n||Tot_17
n||Tot_11=0.0434
n||Tot_12=0.0434
n||Tot_13=0.0434
n||Tot_14=0.0434
n||Tot_16=n||Tot_15
n||Tot_17=n||Tot_16
n||O2_1=n||O2_2
n||O2_1=n||O2_7

```

```

n||CH4_3=n||CH4_4
n||CH4_3=n||CH4_5
x||CO_9=n||CO_9/(n||Tot_9)
x||H2_9=n||H2_9/(n||Tot_9)
x||H2O_9=n||H2O_9/(n||Tot_9)
x||CH4_9=n||CH4_9/(n||Tot_9)
x||CO2_9=n||CO2_9/(n||Tot_9)
x||O2_ci=n||O2_8/n||Tot_10
x||CH4_ci=n||CH4_9/n||Tot_10
x||CO2_ci=n||CO2_9/n||Tot_10
x||CO2_10=x||CO2_ci+0.077*x||CH4_ci+0.077*x||CO_ci
x||H2O_10=x||H2O_ci+0.5*0.077*x||CH4_ci+0.077*x||H2_ci
x||N2_10=n||N2_1/n||Tot_10
x||O2_10=1-(x||CO2_10+x||H2O_10+x||N2_10)
t_1=25
p_1=1.01325
P||comp_r=7
p_2=P||comp_r*p_1
eta||com_mech=0.98
eta||com_isn=0.80
t_3=25
p_3=1.01325
p_4=P||comp_r*p_3
eta||pump_isn=0.80
eta||pump_mech=0.98
t_15=25
t_16=25
p_15=1.01325
P||pmp_r=P||comp_r
p_16=P||pmp_r*p_15
pTur_e=0.18
p_11=1.2
eta||isn_Tur=0.80
eta||mech_Tur=0.98
epsilon=0.8
eta_comb=0.98
eta_inv=0.950
t_cell=1073
t_8=1073
t_9=1073
K_a=2.13*10^8
K_c=1.49*10^8
E_a=110000
E_c=160000
n_e=2
U_f=0.85
I_L=9000
J=1000
d_m=A*d
A_one_cell=p_i*d_m*L_cell
h||o_H2O=enthalpy(H2O,T=T||C_0)
h||o_H2=enthalpy(H2,T=T||C_0)
h||o_CO=enthalpy(CO,T=T||C_0)
h||o_CH4=enthalpy(CH4,T=T||C_0)
h||o_CO2=enthalpy(CO2,T=T||C_0)
h||o_N2=enthalpy(N2,T=T||C_0)
h||o_O2=enthalpy(O2,T=T||C_0)
h||o_water=enthalpy(Water,T=T||C_0,P=P||0)
s||o_N2=entropy(N2,T=T||C_0,P=P||0)

```

```

s||o_O2=entropy(O2,T=T||C_0,P=P||0)
s||o_CH4=entropy(CH4,T=T||C_0,P=P||0)
s||o_H2O=entropy(H2O,T=T||C_0,P=P||0)
s||o_H2=entropy(H2,T=T||C_0,P=P||0)
s||o_CO=entropy(CO,T=T||C_0,P=P||0)
s||o_CO2=entropy(CO2,T=T||C_0,P=P||0)
h_CO2=enthalpy(CO2,T=t_cell)
h_CO=enthalpy(CO,T=t_cell)
h_CH4=enthalpy(CH4,T=t_cell)
h_water=enthalpy(Water,T=t_cell,P=p_cell)
s_H2O=entropy(H2O,T=t_cell,P=p_cell)
s_O2=entropy(O2,T=t_cell,P=p_cell)
s_H2=entropy(H2,T=t_cell,P=p_cell)
s_CO2=entropy(CO2,T=t_cell,P=p_cell)
s_CO=entropy(CO,T=t_cell,P=p_cell)
s_CH4=entropy(CH4,T=t_cell,P=p_cell)
s_water=entropy(Water,T=t_cell,P=p_cell)
p_10=p_2
p_6=p_2
p_11=p_12
p_12=p_13
p_13=p_14
p_4=p_5
p_7=p_2
p_8=p_10
p_9=p_10
p_17=p_16
rho_a=2.98*10^(-5)*exp(-1392/T||K_cell)
rho_c=8.114*10^(-5)*exp(600/T||K_cell)
rho_e=2.94*10^(-5)*exp(10350/T||K_cell)
rho_i=0.025
R_pt=(epsilon_p/xi)
eta||ohm_ano=(J*rho_a*t_a)
eta||ohm_cat=(J*rho_c*t_c)
eta||ohm_elyt=J*rho_e*t_e
eta||ohm_int=(J*rho_i*t_i)
eta_ohm=eta||ohm_ano+eta||ohm_cat+eta||ohm_elyt+eta||ohm_int
i_oa=k_a*(p_H2/P||0)*(p_H2O/P||0)*exp(-E_a/(R_u*T||K_cell))
i_oc=k_c*((p_O2/P||0)^m)*exp(-E_c/(R_u*T||K_cell))
J=i_oa*(exp((alpha*n_e*F*eta_act_ano)/(R_u*T||K_cell))-exp(-((1-alpha)*n_e*F*eta_act_ano)/(R_u*T||K_cell)))
J=i_oc*(exp((alpha*n_e*F*eta_act_cat)/(R_u*T||K_cell))-exp(-((1-alpha)*n_e*F*eta_act_cat)/(R_u*T||K_cell)))
eta_con_cat=-((R_u*T||K_cell)/(4*F))*ln(1-(J/I_L))
eta_con=eta_con_ano+eta_con_cat
E||o=-DELTA_g/(n_e*F)
E||oo=-DELTA_h/(n_e*F)
E=E||o+((R_u*T||K_cell)/(n_e*F))*ln((p_H2*(p_O2)^m)/p_H2O)
SIGMA_ETA=(eta_act+eta_con+eta_ohm)
V_cell=E-SIGMA_ETA
h_8=x||O2_8*enthalpy(O2,T=t_8)+x||N2_8*enthalpy(N2,T=t_8)
h_9=x||H2_9*enthalpy(H2,T=t_9)+x||CO2_9*enthalpy(CO2,T=t_9)+x||CO_9*enthalpy(CO,T=t_9)+x||CH4_9*enthalpy(CH4,T=t_9)+x||H2O_9*enthalpy(H2O,T=t_9)
s||N2_10=entropy(N2,T=t_10,P=p_10)
s||O2_10=entropy(O2,T=t_10,P=p_10)
s||CO2_10=entropy(CO2,T=t_10,P=p_10)
s||H2O_10=entropy(H2O,T=t_10,P=p_10)
s_10=x||N2_10*s||N2_10+x||O2_10*s||O2_10+x||CO2_10*s||CO2_10+x||H2O_10*s||H2O_10
s||N2_11s=entropy(N2,T=t_11s,P=p_11)
s||O2_11s=entropy(O2,T=t_11s,P=p_11)

```

```

s||CO2_11s=entropy(CO2,T=t_11s,P=p_11)
s||H2O_11s=entropy(H2O,T=t_11s,P=p_11)
s_11s=x||N2_10*s||N2_11s+x||O2_10*s||O2_11s+x||CO2_10*s||CO2_11s+x||H2O_10*s||H2O_11s
h_11s=x||N2_10*enthalpy(N2,T=t_11s)+x||O2_10*enthalpy(O2,T=t_11s)+x||CO2_10*enthalpy(CO2,T=t_11s)+
x||H2O_10*enthalpy(H2O,T=t_11s)
eta||isn_Tur*(h_10-h_11s)=(h_10-h_11)
h_11=x||N2_10*enthalpy(N2,T=t_11)+x||O2_10*enthalpy(O2,T=t_11)+x||CO2_10*enthalpy(CO2,T=t_11)+x||H
2O_10*enthalpy(H2O,T=t_11)
s||N2_11=entropy(N2,T=t_11,P=p_11)
s||O2_11=entropy(O2,T=t_11,P=p_11)
s||CO2_11=entropy(CO2,T=t_11,P=p_11)
s||H2O_11=entropy(H2O,T=t_11,P=p_11)
s_11=x||N2_10*s||N2_11+x||O2_10*s||O2_11+x||CO2_10*s||CO2_11+x||H2O_10*s||H2O_11
s||gen_10_11=s_11-s_10
h||o_10=x||N2_10*h||o_N2+x||O2_10*h||o_O2+x||CO2_10*h||o_CO2+x||H2O_10*h||o_H2O
s||o_10=x||N2_10*s||o_N2+x||O2_10*s||o_O2+x||CO2_10*s||o_CO2+x||H2O_10*s||o_H2O
ex||ph_10=h_10-h||o_10-T||0*(s_10-s||o_10)
h||o_11=h||o_10
s||o_11=s||o_10
ex||ph_11=h_11-h||o_11-T||0*(s_11-s||o_11)
w_Tur=(h_10-h_11)*eta||mech_Tur
h_1=x||N2_1*enthalpy(N2,T=t_1)+x||O2_1*enthalpy(O2,T=t_1)
s||N2_1=entropy(N2,T=t_1,P=p_1)
s||O2_1=entropy(O2,T=t_1,P=p_1)
s_1=x||N2_1*s||N2_1+x||O2_1*s||O2_1
s_2s=s_1
s||N2_2s=entropy(N2,T=t_2s,P=p_2)
s||O2_2s=entropy(O2,T=t_2s,P=p_2)
s_2s=x||N2_1*s||N2_2s+x||O2_1*s||O2_2s
h_2s=x||N2_1*enthalpy(N2,T=t_2s)+x||O2_1*enthalpy(O2,T=t_2s)
eta||com_isn*(h_2-h_1)=(h_2s-h_1)
h_2=x||N2_1*enthalpy(N2,T=t_2)+x||O2_1*enthalpy(O2,T=t_2)
s||N2_2=entropy(N2,T=t_2,P=p_2)
s||O2_2=entropy(O2,T=t_2,P=p_2)
s||gen_1_2=s_2-s_1
s||o_1=x||N2_1*s||o_N2+x||O2_1*s||o_O2
h||o_1=x||N2_1*h||o_N2+x||O2_1*h||o_O2
ex||ph_1=(h_1-h||o_1)-T||0*(s_1-s||o_1)
h||o_2=h||o_1
ex||ph_2=(h_2-h||o_2)-T||0*(s_2-s||o_2)
h_3=x||CH4_3*enthalpy(CH4,T=t_1)
s||CH4_3=entropy(CH4,T=t_3,P=p_3)
s_3=x||CH4_3*s||CH4_3
s_4s=s_3
s||CH4_4s=entropy(CH4,T=t_4s,P=p_4)
s_4s=x||CH4_3*s||CH4_4s
h_4s=x||CH4_3*enthalpy(CH4,T=t_4s)
eta||com_isn*(h_4-h_3)=(h_4s-h_3)
h_4=x||CH4_3*enthalpy(CH4,T=t_4)
s||CH4_4=entropy(CH4,T=t_4,P=p_4)
s_4=x||CH4_3*s||CH4_4
s||gen_3_4=s_4-s_3
h||o_3=x||CH4_3*h||o_CH4
s||o_3=x||CH4_3*s||o_CH4
ex||ph_3=h_3-h||o_3-T||0*(s_3-s||o_3)
h||o_4=h||o_3
s||o_4=s||o_3
ex||ph_4=h_4-h||o_4-T||0*(s_4-s||o_4)
w||fuel_com=(h_3-h_4)/eta||com_mech

```

```

h_15=enthalpy(Water,T=t_15,P=p_15)
s||water_15=entropy(Water,T=t_15,P=p_15)
s_15=x||water_15*s||water_15
s_16s=s_15
s||water_16s=entropy(Water,T=t_16s,P=p_16)
s_16s=x||water_15*s||water_16s
h_16s=x||water_15*enthalpy(Water,T=t_16s,P=p_16)
s||water_16=entropy(Water,T=t_16,P=p_16)
s_16=x||water_15*s||water_16
V_15=volume(Water,T=t_15,P=p_15)
w_p=-V_15*100*(p_16-p_15)
h_7=x||O2_1*enthalpy(O2,T=t_7)+x||N2_1*enthalpy(N2,T=t_7)
n||Tot_10*(h_11-h_12)=n||Tot_1*(h_7-h_2)
h_12=x||N2_10*enthalpy(N2,T=t_12)+x||O2_10*enthalpy(O2,T=t_12)+x||CO2_10*enthalpy(CO2,T=t_12)+x||H2O_10*enthalpy(H2O,T=t_12)
h_5=x||CH4_3*enthalpy(CH4,T=t_5)
n||Tot_10*(h_12-h_13)=n||CH4_3*(h_5-h_4)
h_13=x||N2_10*enthalpy(N2,T=t_13)+x||O2_10*enthalpy(O2,T=t_13)+x||CO2_10*enthalpy(CO2,T=t_13)+x||H2O_10*enthalpy(H2O,T=t_13)
h_17=x||H2O_17*enthalpy(Water,T=t_17,P=p_17)
n||Tot_10*(h_13-h_14)=n||water_15*(h_17-h_16)
h_14=x||N2_10*enthalpy(N2,T=t_14)+x||O2_10*enthalpy(O2,T=t_14)+x||CO2_10*enthalpy(CO2,T=t_14)+x||H2O_10*enthalpy(H2O,T=t_14)
s_5=x||CH4_5*s||CH4_5
s||CH4_5=entropy(CH4,T=t_5,P=p_4)
s_17=x||H2O_17*s||H2O_17
s||H2O_17=entropy(Steam,T=t_17,P=p_17)
s||CH4_6=entropy(CH4,T=t_6,P=p_6)
s||H2O_6=entropy(Steam,T=t_6,P=p_6)
s_6=x||CH4_6*s||CH4_6+x||H2O_6*s||H2O_6
h_6=x||CH4_6*enthalpy(CH4,T=t_6)+x||H2O_6*enthalpy(Steam,T=t_6,P=p_6)
h||o_12=h||o_11
s||o_12=s||o_11
s_12=x||N2_10*entropy(N2,T=t_12,P=p_11)+x||O2_10*entropy(O2,T=t_12,P=p_11)+x||CO2_10*entropy(CO2,T=t_12,P=p_11)+x||H2O_10*entropy(H2O,T=t_12,P=p_12)
ex||ph_12=(h_12-h||o_12)-T||0*(s_12-s||o_12)
h||o_13=h||o_12
s||o_13=s||o_12
s_13=x||N2_10*entropy(N2,T=t_13,P=p_11)+x||O2_10*entropy(O2,T=t_13,P=p_11)+x||CO2_10*entropy(CO2,T=t_13,P=p_11)+x||H2O_10*entropy(H2O,T=t_13,P=p_13)
ex||ph_13=(h_13-h||o_13)-T||0*(s_13-s||o_13)
h||o_14=h||o_13
s||o_14=s||o_13
s_14=x||N2_10*entropy(N2,T=t_14,P=p_11)+x||O2_10*entropy(O2,T=t_14,P=p_11)+x||CO2_10*entropy(CO2,T=t_14,P=p_11)+x||H2O_10*entropy(H2O,T=t_14,P=p_14)
ex||ph_14=(h_14-h||o_14)-T||0*(s_14-s||o_14)
h||o_15=h||o_water
s||o_15=s||o_water
ex||ph_15=(h_15-h||o_15)-T||0*(s_15-s||o_15)
h||o_16=h||o_15
s||o_16=s||o_15
ex||ph_16=(h_16-h||o_15)-T||0*(s_16-s||o_15)
h||o_17=h||o_H2Os
s||o_17=s||o_H2Os
ex||ph_17=(h_17-h||o_17)-T||0*(s_17-s||o_17)
x||CH4_5=x||CH4_3
s||o_5=x||CH4_5*s||o_CH4
h||o_5=x||CH4_5*h||o_CH4
ex||ph_5=(h_5-h||o_5)-T||0*(s_5-s||o_5)

```



$h|o_6=x|CH4_6*h|o_{CH4+x}|H2O_6*h|o_{H2Os}$   
 $s|o_6=x|CH4_6*s|o_{CH4+x}|H2O_6*s|o_{H2Os}$   
 $ex|ph_6=h_6-h|o_6-T|0*(s_6-s|o_6)$   
 $h|o_7=h|o_1$   
 $s|o_7=s|o_1$   
 $s_7=x|N2_1*entropy(N2,T=t_7,P=p_7)+x|O2_1*entropy(O2,T=t_7,P=p_7)$   
 $ex|ph_7=(h_7-h|o_7)-T|0*(s_7-s|o_7)$   
 $s|o_8=x|O2_8*s|o_{O2+x}|N2_8*s|o_{N2}$   
 $s_8=x|N2_8*entropy(N2,T=t_8,P=p_8)+x|O2_8*entropy(O2,T=t_8,P=p_8)$   
 $h|o_8=x|O2_8*h|o_{O2+x}|N2_8*h|o_{N2}$   
 $ex|ph_8=(h_8-h|o_8)-T|0*(s_8-s|o_8)$   
 $s|o_9=x|H2_9*s|o_{H2+x}|CO2_9*s|o_{CO2+x}|CO_9*s|o_{CO+x}|CH4_9*s|o_{CH4+x}|H2O_9*s|o_{H2O}$   
 $s_9=x|H2_9*entropy(H2,T=t_9,P=p_9)+x|CO2_9*entropy(CO2,T=t_9,P=p_9)+x|CO_9*entropy(CO,T=t_9,P=p_9)+x|CH4_9*entropy(CH4,T=t_9,P=p_9)+x|H2O_9*entropy(H2O,T=t_9,P=p_9)$   
 $h|o_9=x|H2_9*h|o_{H2+x}|CO2_9*h|o_{CO2+x}|CO_9*h|o_{CO+x}|CH4_9*h|o_{CH4+x}|H2O_9*h|o_{H2O}$   
 $ex|ph_9=h_9-h|o_9-T|0*(s_9-s|o_9)$   
 $ex|ch_1=x|N2_1*ex|ch_{N2+x}|O2_1*ex|ch_{O2}$   
 $ex|ch_2=ex|ch_1$   
 $ex|ch_7=ex|ch_2$   
 $ex|ch_3=x|CH4_3*ex|ch_{CH4}$   
 $ex|ch_4=ex|ch_3$   
 $ex|ch_5=ex|ch_4$   
 $ex|ch_6=x|CH4_6*ex|ch_{CH4+x}|H2O_6*ex|ch_{H2O}$   
 $ex|ch_{12}=ex|ch_{11}$   
 $ex|ch_{13}=ex|ch_{12}$   
 $ex|ch_{14}=ex|ch_{13}$   
 $ex|ch_{15}=ex|ch_{water}$   
 $ex|ch_{16}=ex|ch_{15}$   
 $ex|ch_{17}=ex|ch_{H2O}$   
 $P|DC=V_{cell}*I$   
 $P|AC=P|DC*eta_{inv}$   
 $w|Tur_{net}=n|Tot_{10}*w_{Tur}+(n|Tot_1*w|air_{com}+n|CH4_3*w|fuel_{com}+n|water_{15}*w_p)$   
 $w|Tur_{elec}=eta_{gen}*w|Tur_{net}$   
 $w|Elec_{net}=w|Tur_{elec}+P|AC$   
 $eta|Plant_{elec\_I}=100*w|Elec_{net}/(n|CH4_3*LHV|CH4)$   
 $P_d=J*V_{cell}$   
 $eta|Plant_{elec\_II}=100*w|Elec_{net}/(E_1+E_3+E_{15})$   
 $ex_1=ex|ch_1+ex|ph_1$   
 $E_1=n|Tot_1*ex_1$   
 $ex_2=ex|ch_2+ex|ph_2$   
 $E_2=n|Tot_2*ex_2$   
 $ex_3=ex|ch_3+ex|ph_3$   
 $E_3=n|Tot_3*ex_3$   
 $ex_4=ex|ch_4+ex|ph_4$   
 $E_4=n|Tot_4*ex_4$   
 $ex_5=ex|ch_5+ex|ph_5$   
 $E_5=n|Tot_5*ex_5$   
 $ex_6=ex|ch_6+ex|ph_6$   
 $E_6=n|Tot_6*ex_6$   
 $ex_7=ex|ch_7+ex|ph_7$   
 $E_7=n|Tot_7*ex_7$   
 $ex_8=ex|ch_8+ex|ph_8$   
 $E_8=n|Tot_8*ex_8$   
 $ex_9=ex|ch_9+ex|ph_9$   
 $E_9=n|Tot_9*ex_9$   
 $ex_{10}=ex|ch_{10}+ex|ph_{10}$   
 $E_{10}=n|Tot_{10}*ex_{10}$   
 $ex_{11}=ex|ch_{11}+ex|ph_{11}$   
 $E_{11}=n|Tot_{11}*ex_{11}$

$ex_{12} = ex|ch_{12} + ex|ph_{12}$   
 $E_{12} = n|Tot_{12} * ex_{12}$   
 $ex_{13} = ex|ch_{13} + ex|ph_{13}$   
 $E_{13} = n|Tot_{13} * ex_{13}$   
 $ex_{14} = ex|ch_{14} + ex|ph_{14}$   
 $E_{14} = n|Tot_{14} * ex_{14}$   
 $ex_{15} = ex|ch_{15} + ex|ph_{15}$   
 $E_{15} = n|Tot_{15} * ex_{15}$   
 $E_{17} = n|Tot_{17} * ex_{17}$   
 $E|com1\_D = E_{1-n}|Tot_{1*w}|air\_com - E_2$   
 $E|com2\_D = E_{3-n}|Tot_{3*w}|fuel\_com - E_4$   
 $E|tur\_D = E_{10-n}|Tot_{10} * (h_{10} - h_{11}) - E_{11}$   
 $E|mix\_D = E_5 + E_{17} - E_6$   
 $E|HRSG\_D = E_{16} + E_{13} - (E_{14} + E_{17})$   
 $E|HE1\_D = E_{11} + E_2 - (E_{12} + E_7)$   
 $E|HE2\_D = E_{12} + E_4 - (E_{13} + E_5)$   
 $E|SOFC\_D = E_7 + E_6 - (E_8 + E_9 + P||DC)$   
 $E|CC\_D = E_8 + E_9 - E_{10}$   
 $E|PUMP\_D = E_{16} - E_{15}$